



## Research paper

## Hybrid hydrogen fuel cell and internal combustion engine powertrain arrangements for large maritime applications

Panos Manias<sup>a,b,\*</sup>, Damon A.H. Teagle<sup>b,c</sup>, Dominic Hudson<sup>a</sup>, Stephen Turnock<sup>a</sup><sup>a</sup> University of Southampton, Maritime Engineering, UK<sup>b</sup> University of Southampton, Southampton Marine & Maritime Institute, UK<sup>c</sup> University of Southampton, School of Ocean and Earth Science, UK

## ARTICLE INFO

## Keywords:

Hydrogen  
Decarbonisation  
Shipping  
Net-zero  
Efficiency  
Fuel cells  
Combustion  
Batteries  
Hybrids

## ABSTRACT

Hydrogen as a maritime fuel can be used both in internal combustion engines (HyICE) and with fuel cells (FC). Batteries are required for FC to mediate load fluctuations and can be used with HyICE to reduce installed capacity at the cost of added mass and volume. This study compares the energy efficiency, mass and volume requirements for four hybrid configurations of hydrogen FCs, ICE, and batteries benchmarked against a direct drive diesel ICE. A 136.1 m long, 17.65 MW installed power, 1700 passenger ferry operating a 220 nautical mile liner service is chosen as a representative ship with a total voyage energy demand of 0.51 TJ. Such vessels are likely to provide a starting point in shipping fuel transition to zero carbon as mandated by the International Maritime Organisation. The comparative analysis uses recorded time-domain voyage power demand data and a matching time accurate Python model of the various power train configurations to provide a matching power supply. Results show that HyICE–battery systems achieve ~49 % efficiency. The FC–battery hybrid has the highest efficiency (~54 %). A triple hybrid of HyICE, FC, and batteries reduces battery capacity, mass, and volume by 72 % compared to FC–battery systems, without loss of efficiency.

## 1. Introduction

The International Maritime Organisation (IMO) in response to the Paris accord for mitigating global warming, requires shipping to reduce its Greenhouse Gas (GHG) emissions to a net zero carbon footprint by 2050, with intermediate targets in 2030 and 2040 (I.M.O., 2023). Post 2030, this requires ships to use clean fuels which either do not contain carbon or offset carbon emissions at a certain point in their lifecycle, often referred to as zero and net-zero emission fuels respectively. Possible future fuel candidates include green ammonia, methanol and hydrogen with the first two produced using hydrogen thereby requiring a significantly larger renewable energy investment (Manias et al., 2024). The most energy efficient pathways for hydrogen utilisation for maritime applications use fuel cells but these powertrain propositions are relatively untested with only a few operational examples in shipping (Sundén, 2019).

The maritime sector has inherent resistance to change in its power trains due to the imperative need for safe operation with extremely high levels of reliability (Griffiths, 1997). Risks associated with operational safety, equipment reliability, availability of skilled crews and economic

viability, all need to be considered when opting to build new vessels (Psaraftis et al., 2012) as the new ship must be a secure investment that will pay for itself during operations and provide a return on investment (ROI). The long-life span of ships, often 20+ years can be a major barrier whilst optimal future fuel choices remain unclear and debated. Previous transitions: sail to steam; coal to oil; have taken place over many decades. The timeline to meet IMO targets for 2030 is much shorter and hence there is urgent need for confidence in the performance of power trains that use future fuels.

Internal Combustion Engine (ICE) powertrains have propelled most ships for the past century, offering the mandatory high levels of reliability and crew familiarity. In contrast, fuel cells are relatively new to the shipping industry and regarded as untested and costly technology (Xing et al., 2021). Consequently, resistance towards proposed hydrogen-powered Fuel Cell (FC)-battery powertrains as a substitute for traditional ICE is to be expected (McKinlay et al., 2021a; McKinlay et al., 2024/06). Several studies have investigated partial and full refit vessel powertrains considering different arrangements of hydrogen powered fuel cells and batteries (McKinlay et al., 2024/06; Mylonopoulos et al., 2024/11), some in combination with ICE burning fossil fuels (Melideo

\* Corresponding author. University of Southampton, Maritime Engineering, UK.  
E-mail address: [pm2c21@soton.ac.uk](mailto:pm2c21@soton.ac.uk) (P. Manias).

<https://doi.org/10.1016/j.oceaneng.2025.123505>

Received 21 July 2025; Received in revised form 5 November 2025; Accepted 9 November 2025

Available online 17 November 2025

0029-8018/Crown Copyright © 2025 Published by Elsevier Ltd. This is an open access article under the CC BY license (<http://creativecommons.org/licenses/by/4.0/>).

and Desideri, 2024/01). For example, the combination of liquified natural gas (LNG) powered Solid Oxide Fuel Cells (SOFC) with an ICE can be more efficient at meeting shipboard power demands than ICE alone (Micoli et al., 2021), even with the use of LNG. When comparing Hydrogen ICE (HyICE) with fuel cells, Ventayol et al. (2025) suggest that a HyICE powertrain might be a better option from an emissions Lifecycle Assessment perspective. However, although these studies showed increases in energy efficiency with consequent reductions in emissions, no study has examined a combination of FC, HyICE powertrains using the same e-fuel or a powertrain configured to utilise hydrogen most efficiently under different operational criteria, including an optimized combustion method for this fuel. Moreover, studies to date are yet to investigate possible ways of reducing total battery capacity requirements for fuel cell systems or the total installed machinery volume and weight for different powertrain combinations.

The aim of the work is to evaluate which of the possible combination of ICE, FC and batteries provides the most effective power train with respect to overall efficiency, mass and installed volume of the various powertrains. A 136.1 m long, 17.65 MW installed power, 1700 passenger ferry operating a regular 220 nautical mile liner service was chosen as a representative ship. Such ships are seen as potential ‘first movers’ in the transition of the shipping sector as they have known energy demands, ranges and associated bunkering facilities to be developed alongside the shoreside energy supply. Time accurate data (1 Hz) was available for the ship for several voyages and included measurements of power and consumption for the main engines and auxiliary generator systems.

For this work, although decisions on future maritime fuels remain delayed, we have chosen to only consider liquid hydrogen. Similar

analysis could be made for green ammonia or methanol but would change the onboard fuel storage requirements and necessitated increased renewable energy generation (Manias et al., 2024; McKinlay et al., 2024/06). Section 2 provides the background to the future fuel alternatives and justifies the choice of hydrogen for this study. Section 3 details the system level understanding of the power train elements of ICE, FC and batteries necessary to provide a dynamic model that can match the ship’s recorded power demand with the relative balance of outputs from the FC, HyICE and batteries. The overall performance of these elements was benchmarked against the performance of the ship’s actual direct drive diesel engine and generators. The powertrain power supply model development is given in Section 4 along with relevant characteristics of the typical measured voyage and the relevant ship design parameters. Section 5 compares the voyage energy efficiency for the four hybrid powertrains and the benchmark of the actual installed ship powertrain. The required masses and volumes of system components are assessed in Section 6 with the study’s limitations & assumptions in Section 7 and conclusions drawn in Section 8.

## 2. Alternative maritime fuels

Over the course of the past centuries, shipping was required to change its powering source several times. Whether it was from oarsmen and sails to coal or from coal to liquid fuels such as diesel, the principal driving reasons were the needs to reduce costs and reliability coupled to the increased power demands due to increases in ship size, range requirements, and shorter voyage time demands to enable global trade (Fletcher, 1975). Response to the climate emergency will be the first time in maritime history where the incentive to change propulsion

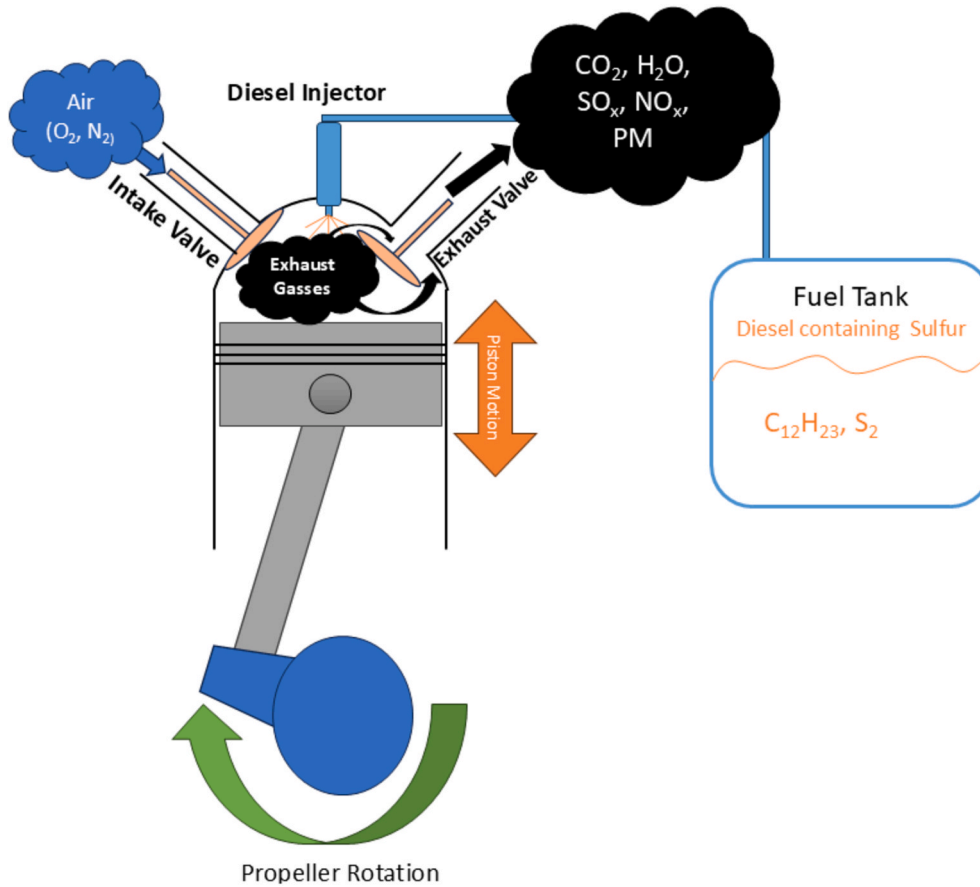


**Fig. 1.** Exhaust gases formed during combustion.  $NO_x$  formation results from the high temperature reaction of atmospheric nitrogen and oxygen, whereas  $SO_x$  result from fuels that include impurities and additives. Particulate Matter (PM) includes soot and other carbonaceous materials resulting from poorly burnt hydrocarbons and commonly contain elevated concentrations of toxic heavy metals (Di Natale and Carotenuto, 2015/10).

methods is driven by environmental sustainability rather than economic drivers, but the latter remain essential considerations for rapid change to occur. It is important to highlight the need to reduce global warming inducing emissions (GHG) should be coupled with the reduction or elimination of other substances such as  $\text{SO}_x$ ,  $\text{NO}_x$  and Particulate Matter (PM) that result from fossil fuel combustion and are detrimental to air quality and human health (Fig. 1).

Such emissions can directly harm human population close to major shipping routes or ports, as funnel emissions can have major impact on local air quality (Gössling et al., 2021/10). Air pollution from such gases is estimated to be responsible for 4.2 million deaths every year ("Ambient"), with shipping contributing as much as ~15 % of global  $\text{NO}_x$  and  $\text{SO}_x$  emissions and 2 % of global particulate matter (PM<sub>2.5</sub>) (Gössling et al., 2021/10).  $\text{SO}_x$  emissions have reduced through the use of higher grade diesel fuel oil with a very low concentration in sulphur or by utilising onboard scrubbers for removing  $\text{SO}_x$  (Yang et al., 2012/08). However, scrubber systems have caused issues to local water quality (Teuchies et al., 2020/07) and are now banned in certain waters (Al Din Al Hajjaji, 2023).  $\text{NO}_x$  emissions have been reduced somewhat by optimising combustion as well as including post-combustion systems such as selective catalytic reduction (Yang et al., 2012/08). Although PM emissions cannot be completely eliminated for carbon based fuels they have been reduced through the utilisation of higher distillation fuel products, alternative lubricants and improved maintenance (Di Natale and Carotenuto, 2015/10).

Considering all the emissions issues rising from combustion of conventional hydrocarbons, a range of alternative fuels have been proposed to power maritime activities, with the principal potential green fuel candidates compared to conventional Marine Gas Oil (MGO) in Table 1.

Ammonia ( $\text{NH}_3$ ) is a major industrial commodity essential for producing fertilizers, plastics, explosives that has been proposed as a carbon-free fuel for heavy plant including shipping ("Ammonia as a marine fuel, 2020; Zamfirescu and Dincer, 2008/10). The molecule contains no carbon and can be used to fuel marine internal combustion engines, when combined with a significant proportion of diesel, the amount of which being dependent upon engine loading factors, requiring between 5 and 15 % of pilot fuel contribution by mass (Lasocki et al., 2019; Scharl, 2022; Mi et al., 2023/07; Xu et al., 2023/10). Ammonia is also a potential feedstock for fuel cells, but significant energy is required to dissociate or 'crack' the ammonia and to purify the hydrogen (Thomas, 2006).  $\text{NH}_3$  is liquid at  $-37^\circ\text{C}$  and contains 45 % more hydrogen molecules per unit of volume compared to liquid  $\text{H}_2$ , making ammonia an attractive hydrogen carrier, with 17.8 % hydrogen

by mass (Aziz et al., 2020). However, ammonia is highly toxic and although a major cryogenic maritime cargo, its safe handling as a marine fuel remains unproven ("ENGINE RETROFIT REPORT, 2023, 2023). Although ammonia can be detected in very small concentrations (5 ppm) in the air, it is colourless and hydrophilic, with a strong pungent odour (Service, 2018). It is lethal when ingested. Due to its toxicity, an ammonia spillage in the environment could severely impact marine biodiversity (Ng et al., 2023/06). The use of ammonia as a maritime fuel may be unacceptable to the general public (Carlisle et al., 2023) especially if large bunkers are stored in port cities.

Methanol ( $\text{CH}_3\text{OH}$ ) is also considered as a future maritime fuel ("Methanol for the maritime energy), despite still having  $\text{CO}_2$  tailpipe emissions due to the presence of carbon in the molecule, and that hydrocarbon pilot fuel is required to aid combustion (Liu, 2010). It is liquid in ambient conditions and relatively easy to handle requiring only relatively minor modifications to the current storage and handling equipment used by maritime, such as double walled tanks and special anti-corrosion coatings ("Methanol as an alternative fuel). Methanol can be synthesised from biomass, but growing these feedstocks may compete for land essential for increasing food production or renewable energy (Svanberg et al., 2018/10). Renewable, 'green' methanol can be produced by bonding green hydrogen with  $\text{CO}_2$  removed from the atmosphere via Direct Air Capture (DAC) systems, through the implementation of the Fischer-Tropsch process. Theoretically, this would enable the combustion of methanol to become near net zero with respect to its total emissions footprint after utilisation, but DAC technologies are energy intensive and as yet unproven at industrial scales (Erans et al., 2022; Wilcox et al., 2017).

Although both ammonia and methanol could be utilised via cracking with fuel cells, current industry preference is to burn them in adapted ICE (Mallouppas and Yfantis, 2021). Ammonia combustion reduces ICE efficiency by as much as 5 % at high loads due to its thermochemical properties and subsequent combustion behaviour and relies on fossil fuels to initiate combustion (Førby et al., 2023/01; Niki et al., 2019) producing extremely potent GHG's such as  $\text{N}_2\text{O}$  (Brinks and Hektor, 2020) in addition to  $\text{CO}_2$ . Other pollutants include high levels of  $\text{NO}_x$  (Pedersen et al., 2023/11) and unburnt, toxic ammonia slip (Nadimi et al., 2023/04). Methanol on the other hand, has the potential of increasing thermal efficiency (Karvounis et al., 2023) and can be used with spark ignition more effectively than ammonia due to its high pre-ignition resistance (Wouters et al., 2023/05), yet is prone to formaldehyde formation, which is a carcinogenic gas (Zhang et al., 2011/01).

Hydrogen utilisation is usually promoted through fuel cells

**Table 1**

Key properties of main fuels proposed in the maritime net zero transition. For the Wind to Wake ratio (WtWr), the smaller the ratio of fuel generation energy to fuel exergy the better.

Fuel Type	Conventional		Zero/low carbon		
	MDO (Huang et al., 2021)	LNG (Methane) (Alderman, 2005)	$\text{LH}_2$ (Tashie-Lewis and Nnabuife, 2021/11; Younas et al., 2022/05; Jeon and Kim, 2020)	$\text{LNH}_3$ (Fenton et al., 1995)	Methanol
Density $\rho$ ( $\text{kg}/\text{m}^3$ )	890	440	71	653	780
Lower Calorific Value (LCV) ( $\text{MJ}/\text{kg}$ )	42.8	50	120	18.6	20
Volumetric Energy Density ( $\text{MJ}/\text{L}$ )	38	22	8.5	12.1	15.6
Boiling point ( $^\circ\text{C}$ )	60	-163	-253	-33	64.7
Minimum Embedded Production Energy (per kg)	9 MJ (Hall et al., 2014)	10 MJ (Hall et al., 2014)	170 MJ (Tashie-Lewis and Nnabuife, 2021/11; Younas et al., 2022/05)	43.2 MJ (Pfromm, 2017)	39.6 MJ (Anicic et al., 2014)
Ratio of Energy for Fuel Generation to Fuel exergy (WtWr)	N/A	N/A	1.4:1	2.3:1	2:1
Flammability limits (Air conc. [% v/v])	1.3–6	5–15	4–74	14.8–33.5	6–36.5
Ignition temp. ( $^\circ\text{C}$ )	350–380	537	520	650	433
Hazards	Flammable	Flammable, Cryogenic	Highly Flammable, Cryogenic	Highly Toxic, Cryogenic	Flammable, Toxic Corrosive

(McKinlay et al., 2021a; McKinlay et al., 2024/06) as the higher efficiency powertrain should minimise consumption therefore reducing required storage capacity. Although hydrogen combustion is possible, it also comes with challenges. Primary concerns include the operational safety of the entire H<sub>2</sub> system onboard as well as the additional storage capacity required for the less efficient powertrain. Although some NO<sub>x</sub> emissions can result from the high combustion temperatures attained (Wimmer et al., 2005; Verhelst and Wallner, 2009/12), the primary resulting emission of hydrogen utilisation, either consumed via fuel cells or internal combustions engines, is water vapour.

It is important to note that renewably produced green hydrogen is a requirement for both green ammonia and methanol. Hydrogen is highly volatile and explosive, with a low specific energy density (Baykara, 2018; Kurz et al. et al., 2022). However, the advantage of using hydrogen over its derivatives is based on the amount of renewable energy saved during its production. Liquid hydrogen requires the least amount of renewable energy investment compared to other e-fuels for completing the same maritime relevant activities (30 % less than NH<sub>3</sub> and 26 % less than methanol) (Manias et al., 2024), hence liquid hydrogen is selected as the future fuel of choice for this study.

### 3. Alternative powertrain configurations

#### 3.1. Internal combustion engines

During the late 18th century, fossil fuels grew in favour of renewable energy sources such as wind, as way of powering industry and transport (Sørensen, 1991/01). This was achieved initially through the burning of coal and then liquid fuels such as oil and diesel, when extraction, distillation, supply and utilisation became commercially viable (Melsted and Pallua, 2018).

With cheap and abundant fossil-based energy available, technologies continued to evolve to utilise these substances. This is shown by the relatively slow transition from external combustion steam engines to internal combustion engines that now propel the vast majority of the global fleet (Kennerley, 2008; Paul, 2020) (Fig. 2). As a carryover from the boilers used to burn coal to produce steam and due to familiarity with this technology, the first liquid fuel powered vessels, still used boilers (Flannery, 1925). It is worth noting that the first diesel engines were deemed commercially unviable due to the uncertainty of liquid fuel supply and poor operational reliability compared to coal at the time (1910s) (Flannery, 1925). However, with improvements and experience, later examples were ultimately favoured due to lower running costs

(Charnews, 2009).

Aside from the urgency to address global warming, past maritime technical transitions are similar to today's challenges. Despite the well-established efficiency advantages of FCs, shipping stakeholders still prefer internal combustion engines due to crew familiarity, lower installation costs, and widespread fuel availability through the global bunkering infrastructure. This century-long approach may be continued with the introduction of new combustion fuels such as methanol and ammonia, although both fuels have only rudimentary infrastructure in place, previously being handled as industrial cargos only (Sheldon, 2017; David, 2020).

As with liquid fossil fuels during the early 20th century, hydrogen is treated by many as a non-viable maritime fuel due to lack of availability (Nikolaidis and Poullikkas, 2017), despite its many advantages even as a combustible fuel. This was not always the case, however. As environmental concerns began to rise in the 1970's, the automotive sector promoted hydrogen as a fuel for internal combustion engines (Dell and Bridger, 1975/10; Jones, 1971; Maugh, 1972). Since then, there have been many operational examples, including from Toyota and BMW, of H<sub>2</sub>-fuelled internal combustion engines (Sutton, 2023). However, the additional fuel storage requirements, lack of refuelling infrastructure, and the challenges of controlling combustion at different engine loads (Meyer and Winebrake, 2009; Muratori et al., 2018) has inhibited the uptake of H<sub>2</sub> for vehicles, until recently, with numerous on road commercial applications promoting hydrogen fuelling (Camacho et al., 2022/08).

Hydrogen Internal Combustion Engines (HyICE) may have benefits. Although convenient to use port injection, the more complicated and efficient, direct injection of hydrogen, forming a heterogeneous final mixture that is ignited via spark, can yield thermal efficiencies over 46 % (Boretti, 2020/09). Some arrangements using preignition chambers exceed 50 % thermal efficiencies (Boretti et al., 2010a). Injection at very low temperatures compared to other fuels, due to the conversion of state from storage as a liquid to gas upon the point of injection, hydrogen can also offer a cooling effect within the cylinder (White et al., 2006/08), giving the opportunity of reaching over 50 % thermal efficiency in internal combustion engines (White et al., 2006/08). As a result, the thermal efficiency of HyICEs can come close to efficiencies of a Proton Exchange Membrane (PEM) fuel cell powertrain (minimum 55 %). However, as hydrogen combustion poses many challenges, these high efficiencies are only achievable under specific operational conditions and optimal engine loadings. These include, pre-ignition at low loads (Welch and Wallace, 1990), high NO<sub>x</sub> emissions at lean air fuel ratios

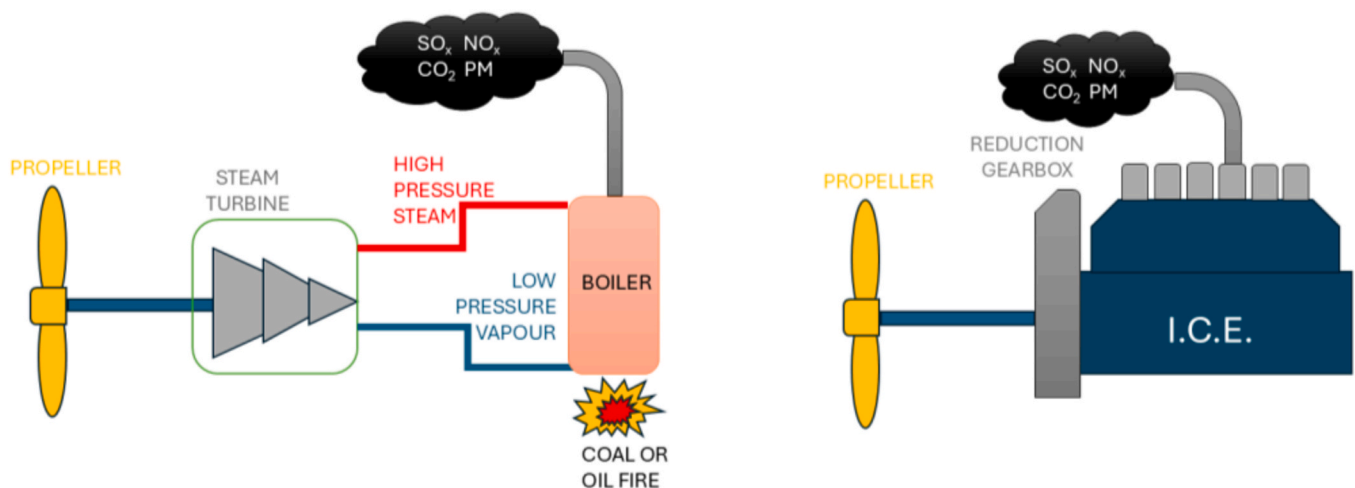


Fig. 2. Initial use of fossil fuels within maritime industry was achieved via steam production onboard by heating water through the combustion of fuels externally of the propulsion system (left). For a more efficient utilisation of the same fuels, the industry switched to Internal Combustion Engines, reducing the fuel consumption and operational costs significantly (right).

(Wimmer et al., 2005), and combustion chamber heat spots due to the fuel mixture's dispersion behaviour (Lee et al., 1995/04; Shudo, 2007/12). However, these issues can be addressed by running HyICE at steady load conditions, such as when used to power an electricity generator. An exhaust catalytic reduction system (Fumey et al., 2018/03), similar to current NO<sub>x</sub> reduction methods can be employed onboard (Bayramoğlu et al., 2024/05), leaving water vapour as the sole exhaust gas emission (Boretti, 2020/09).

### 3.2. Fuel cell powertrains

Fuel cells as a technology, have been in existence for approximately the same amount of time as the concept of internal combustion (Larminie et al., 2003). The main benefit of FCs is the ability to utilise non-carbon containing fuels, as their primary energy source. This technology is based on electrochemical principles instead of combustion and give fuel cells significant efficiency advantages ("Fuel Cells for Shipping, 2021; "Analysing the possibilities of using, 2016). Fig. 3 shows the operational principles of a fuel cell. One important consideration is the need for hydrogen fuel to be in gaseous state, with its pressure feed being within the range of ~5–15 bar and close to ambient temperature, while the air intake must be purified (Larminie et al., 2003). Both operational conditions are assumed to take place for the case studies examined later, as well as to be part of the overall Balance of Plant (BoP), therefore taken into account when considering fuel consumption and efficiency (PemGen MT). An important consideration for hydrogen utilisation through FCs, is the necessity for load levelling batteries (Kersey et al., 2022), which act as a buffer for rapid changes in onboard power demand with FC having relative slow rates of power ramp up/down in comparison with ICE.

Fuel cells are electrochemical devices which require precise control of fluid flow, in both air and fuel intakes which form the anode and cathode sides depending on type (Laboratory and Energy, 2005). Of even greater importance is the electrolyte used, which can be a ceramic made from solid oxide compounds (SOFC) or an electrolytic membrane (PEMFC), that conducts anions and cations through each fuel cell type, allowing for the development of potential difference across the electrodes (Fig. 3).

SOFCs are very sensitive to rapid load fluctuations, as these can damage the ceramic electrolytic structure leading to total system failure (Bhattacharyya and Rengaswamy, 2009/07). PEMFCs can fluctuate their power output at a higher rate, provided the electrolyte's relative humidity is maintained at acceptable levels (Tang et al., 2010/04). However, both FC types require batteries to assist with rapid increases in loads (Szalek et al., 2021; Pagliaro et al., 2020). In contrast, ICE, including hydrogen fuelled systems, have fast responses to varying loads

as thermochemical combustion occurs within milliseconds (Khoja and Lim, 2022; Taylor, 1985). Although they have fast responses, batteries present other challenges that need to be assessed including increased volume and mass requirements alongside significant capital costs. Due to the discharging rate limitations imposed on the batteries (Ning et al., 2003/05; Vega-Garita et al., 2024), a larger charge capacity is expected for battery installation when employed alongside SOFCs, compared to PEMFCs. As such, SOFCs will not be considered in this study.

Heat losses occur whenever there is an energy change of state. This is the case when charging and discharging batteries, as electricity is converted to chemical energy and vice versa. The charging energy loss expected is between 3 and 5 %, bringing the overall system efficiency value of PEM with batteries (55 % on average) closer to HyICE (~50 %). Consequently, an aim of this study is to examine whether the use of a combined HyICE and FC electric powertrain (Fig. 4) could achieve higher efficiencies, in combination with a reduced battery capacity. We also consider whether including additional redundancy to a marine powertrain may enable the transition to a new era of maritime fuels and subsequent powertrains innovations.

### 4. Powertrain power supply model

Here we assess the energy supply requirements for a specified energy demand to propel the ship using a time-domain-based model, coded in Python, of powertrain operation. The same methodology and approach have been used previously to evaluate several vessel case studies and types (McKinlay et al., 2021b, 2022a, 2022b). Fig. 5 illustrates the adopted modelling approach and the application of the time response model equations discussed later.

One second time step (1Hz) recordings allow the detailed evaluation of the time responses of the various components, with resulting data gathered including power and fuel consumption recordings. This approach allows the comparison of different powertrains that comprise components with different response rates, efficiencies, loading factors and physical properties (i.e., size and mass of installed powertrain). The power systems evaluated involve different permutations of the arrangement illustrated in Fig. 4 and are detailed in Table 2. Sizing of individual components is based initially on the vessel's confidential machinery particulars and later optimized through an iterative approach. Although we use a specific vessel as a virtual testbed for the alternative powertrains, our findings are applicable across a wide range of ship types and sizes with variations in the relative balance of components dependent on the duty cycle of the ship including operational conditions such as manoeuvring, steady sailing and port idle.

A full systems diagram (Fig. 6) illustrates how each power supply unit is controlled via an onboard main distribution centre, similar to

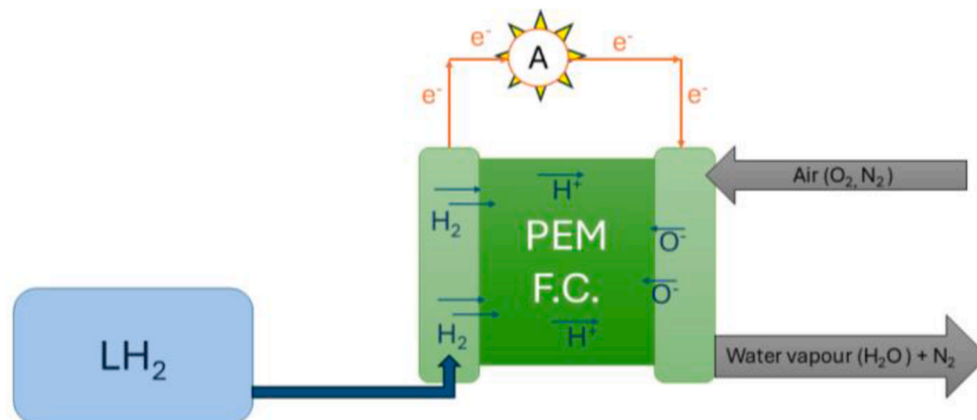


Fig. 3. Illustration of PEM FC operating principles, where fuel (hydrogen) is fed to the anode, oxygen is supplied to the cathode, and electrochemical reactions occur to produce electricity.

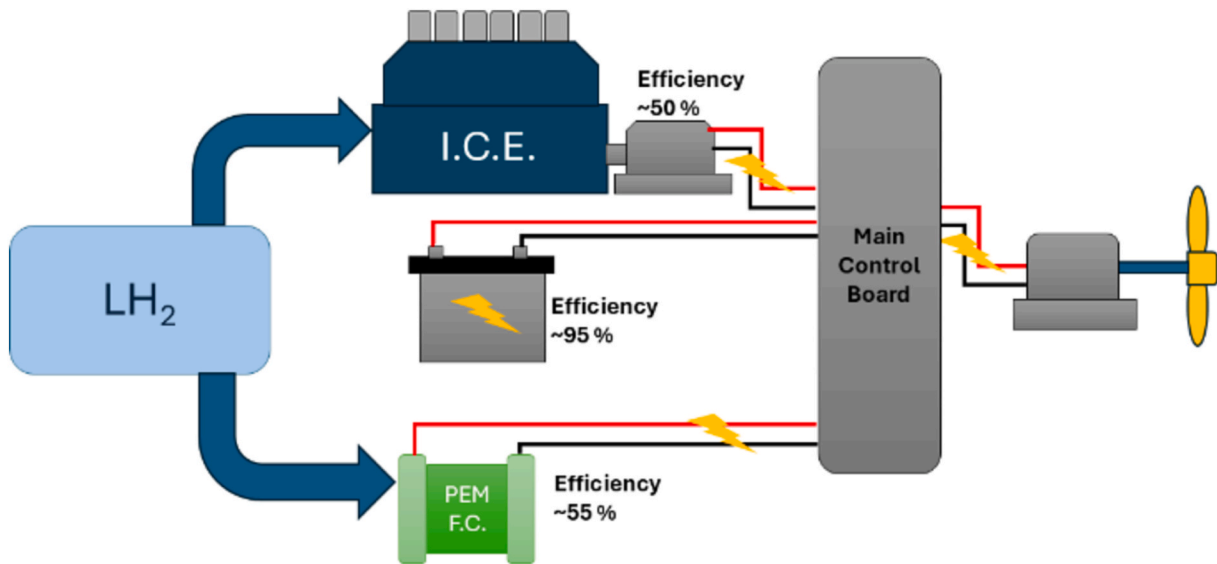


Fig. 4. One of the powertrain configurations proposed in this paper, comprising a HyICE, fuel cells and a small 'buffer' battery.

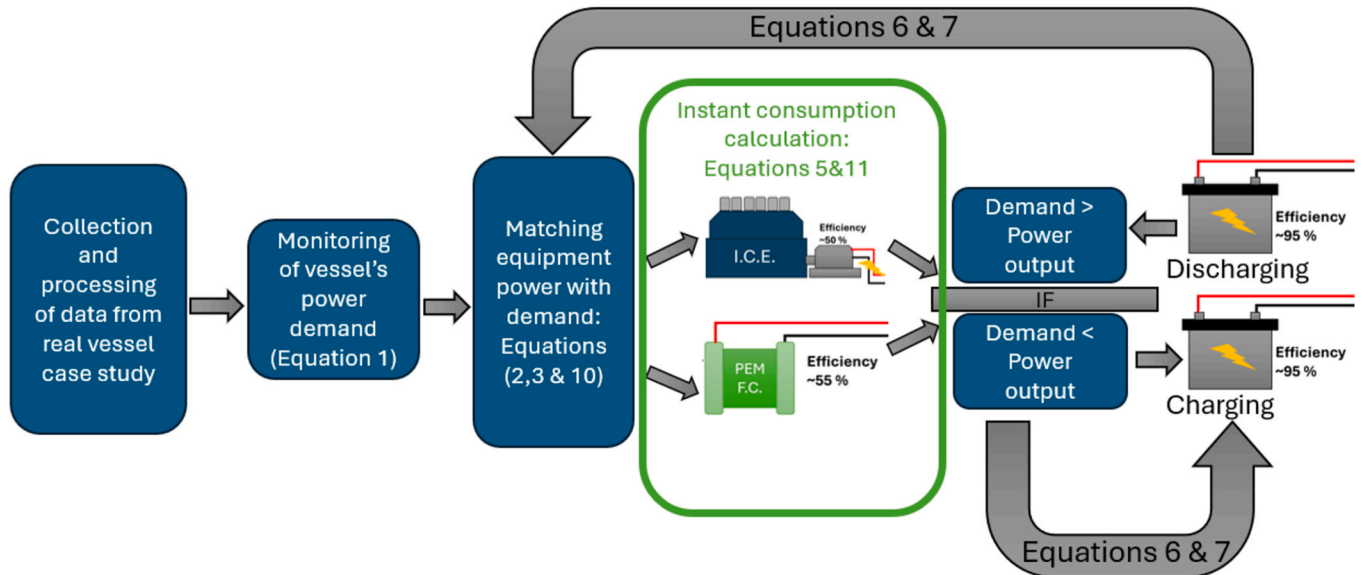


Fig. 5. Illustration of powertrain simulation code operation in real time. Starting with a processable data format, the simulation code monitors the ongoing power demand, according to a set time interval  $n$ . It then decides according to the demand and powertrain system selected, which component will respond first to the onboard power demand change. This is achieved via the implementation of "if" loops. Any excess power is used to charge the batteries, while the battery state of charge is constantly monitored. If the battery completely discharges, the simulation fails and individual components are resized accordingly.

current powertrain hybrid systems currently in service (Hinić et al., 2025/01).

#### 4.1. Case study vessel

Many of the current maritime decarbonisation technology demonstrators are being deployed on short voyages, with preset and recurring routes (Hansen). Such vessels are small cargo carriers or passenger ferries (Pagliaro et al., 2020) with established bunkering infrastructure (Laasma et al., 2022) to assuage fuel supply risks. In this case study, we consider the operations of a passenger ferry currently serving the Aegean Sea on a route between the main port of Athens, Piraeus, and the central Cyclades (Table 3).

Passenger vessels have high power demands compared to other vessel types of similar size (McKinlay, 2023). Fig. 7 displays a typical example of the power demand recorded for the round-trip voyage using

the onboard vessel monitoring system. This representative voyage recording is similar to the annual average value for this vessel on this route, with the total energy demand and subsequent fuel consumption varying by less than  $\pm 10\%$  during the 150 voyage recordings gathered.

Although we will not evaluate the overall total machinery space requirements, we do compare the batteries and HyICE generator sets in terms of their required space and weight. Using the power recordings gathered (Fig. 7), the total voyage energy demand was calculated by multiplying each power recording with the increment amount of time step between readings, giving a cumulative total energy required of 514.4 GJ for each round-trip voyage.

#### 4.2. Data filtering

Batteries are often the first responder to increased electricity demands. As such, different operational strategies can be used for the

**Table 2**  
Powertrain configurations examined.

Scenario	Powertrain Type	Powertrain Specifications	Fuel Type
0	Original Powertrain	4x Diesel Main Engines (17.7 MW) 4x Diesel Generators for auxiliary demand (2.5 MWe)	Diesel
1	HyICE Gensets	4x Hydrogen Combustion Generators (18 MWe)	Liquid Hydrogen
2	HyICE Gensets&Batteries	4x Hydrogen Combustion Generators (18 MWe) Marine battery pack 2.5 MWhe	Liquid Hydrogen
3	PEM Fuel Cells&Batteries	30x Hydrogen PEM Fuel cell stacks (18 MWe) Marine battery pack 2.5 MWhe	Liquid Hydrogen
4	PEM Fuel Cells with HyICE Gensets& Batteries	30x Hydrogen PEM Fuel cell stacks (18 MWe) 2.0 MWe HyICE Genset Marine battery pack 700 kWhe	Liquid Hydrogen

power supply equipment on board, specifically when coupled with fuel cells. These can either operate in a steady state mode or be set-up to run in a dynamic load following manner where the FCs maintain the batteries at a specific level of charge. As also highlighted in a recent study carried out by Mylonopoulos and colleagues, batteries can be considered as buffers and the entire powertrain can be interpreted as operating through the presence of a low pass filter (Mylonopoulos et al., 2024/11).

We follow a similar approach to Swider and Pedersen (Swider and Pedersen, 2018) who investigated recordings of maritime power requirements by applying a fast Fourier transform function to smooth the power signal and better evaluate the energy demands of a vessel. The same function returns the Power Spectral Density (PSD) for every given frequency in the data collected (Fig. 8) which captures the dominant frequencies, by identifying their intensity within the power demand signal. Major power changes with respect to the different operational profiles the vessel undergoes, are expected to be of low frequency throughout the vessel's voyage (Swider and Pedersen, 2018), for example when arriving at port where the vessel switches operational profile from cruising to manoeuvring.

The round-trip voyage examined takes more than 15 h and the vessel makes 5 port calls, with the final port call being the port of origin

(Piraeus, Athens). The frequency (in Hz) through which the total propulsion demand varies, because of these port calls, is therefore expected to be very low. This allows for the implementation of a low pass filter on the power recording data, to capture this load variation. The same filter will remove all signal frequencies above the frequency identified through the FFT function. Such high frequency signals include power changes occurring as a result of the recorder's margin of error or DC to AC converter noise occurring onboard due to the generator sets, further supporting the idea of implementing a low pass filter (Mylonopoulos et al., 2024/11; Swider and Pedersen, 2018). The inclusion of the 0.03 Hz filter does not affect the total energy demand yielding the same final value of 514 GJ (Fig. 9) with or without the filter.

#### 4.3. Fuel cell simulations

The operational code used to examine the fuel cell response to power demand onboard the vessel, is state based on a time domain (Manias et al., 2024; McKinlay et al., 2024/06). This means battery state of charge and the power output of the fuel cells (and later HyICE) are evaluated throughout the voyage. The code captures the power ramp rates of all electrical supply equipment and considers their respective

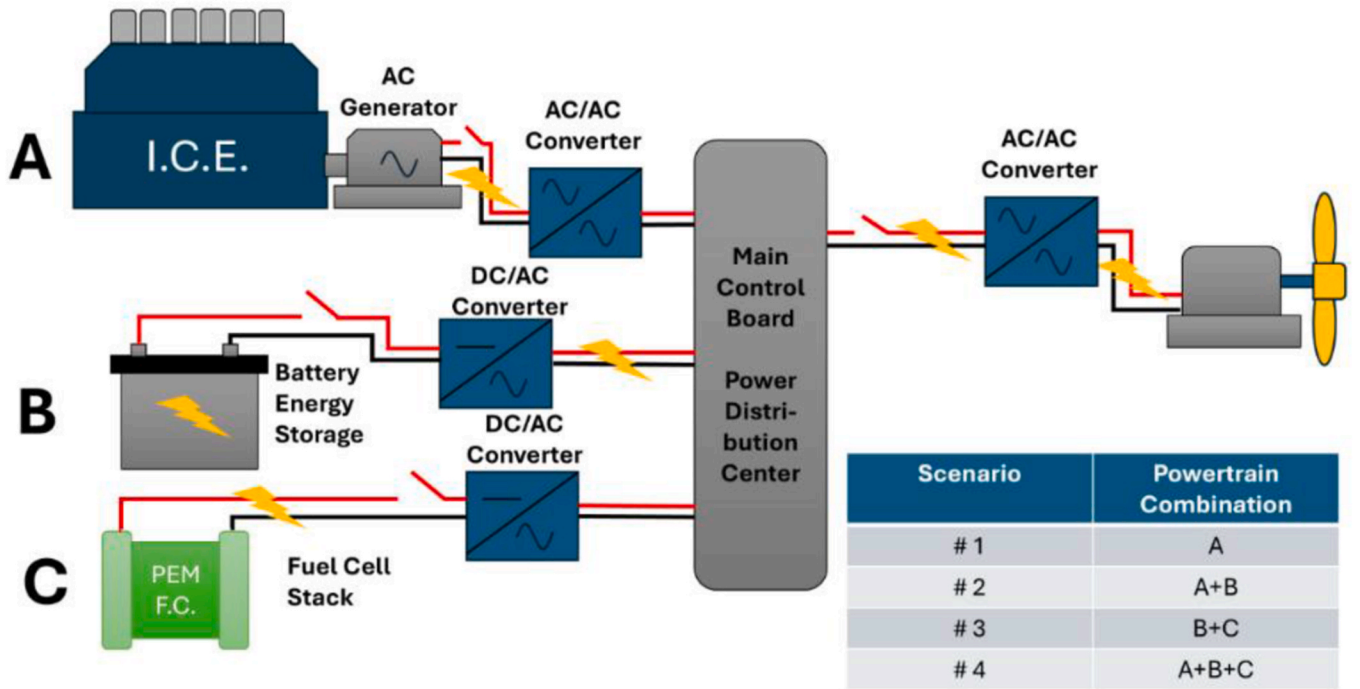


**Fig. 6.** Systems diagram of triple hybrid powertrain proposed with other powertrain configurations considered being different combinations of the main equipment, as specified in Table 2. Note that it is expected that the vessel's main electricity distribution will be provided via Alternating Current, the voltage of which will be defined according to the manufacturers' specifications. HyICE are expected to be started first and then engaged with the grid, once their RPM are matched with the manufacturer specifications to provide the AC frequency required. Fuel Cells and Batteries produce electricity in Direct Current form, necessitating the use of AC converters. At the same time, fuel cells are expected to be operated all the time even, when not producing power, by being in standby mode, yet not connected to the local grid. Total electrical efficiency loss of the system is expected to be no more than 5 % (Dedes et al., 2016).

**Table 3**  
Key characteristics of vessel case study.

Type	Cruise ferry (Ice class)
Tonnage	16,850 Gt
Length	136.1 m
Beam	24.2 m
Draft	5.4 m
Propulsion & Auxiliary	4 × S.M.T.-Pielstick 12PC2-2V 17.65 MW (claimed), with reduction boxes and Controllable Pitch Propeller 4 x Wärtsilä-Vasa 24 2.5 MW
Speed	22 kts max speed 18 kts service speed
Capacity	1,700 passengers 1,184 passenger beds 350 vehicles

efficiencies (Fig. 10).

The consumption of the fuel cells is based on the load they are subjected to, at each time step. Fig. 11 illustrates an example of the different power output responses expected from each powertrain component.

Depending on the power demand on board, the target power,  $P_{Target}$  output for the fuel cells is altered. The target power for the fuel cell (equation (1)), is initially set according to the on-going demand, where the time step for the code's domain is set according to the desired operational mode (steady state or dynamic load following).

$$P_{Target} = avg(P_C, P_{C-n}) \quad (1)$$

Where:  $P_C$  is the power at the time of interest processed within the main code;  $P_{C-n}$  is the power recording processed  $n$  seconds ago. Fuel cells can operate in either dynamic following mode or steady state, depending on the time interval  $n$ , as the frequency of change in the target power is initially set by  $n$  and then according to the batteries' state of charge.

The following empirical curve fit equations are used within the code

to match the power ramp rates and fuel consumption, using data made available by a marine fuel cell manufacturer (Marine power generation system 200) and battery characteristics provided by relevant literature reviews (McKinlay et al., 2024/06; Kaur et al., 2022):

$$P_{Battery} = P_{max} * \tanh(0.5 * t) \quad (2)$$

$$P_{FuelCell} = P_{max} * \tanh(0.12 * t^{0.8}) \quad (3)$$

where:  $t$  is time (s);  $P_{Battery}$  is the power output for a battery (kW), which is expected to be limited by 3 times its total charge capacity ( $C$ ) for the charging and discharging rate for the battery type selected (Ning et al., 2003/05; Vega-Garita et al., 2024);  $P_{FuelCell}$  is the power output for a fuel cell (kW);  $P_{max}$  is the maximum rated power of the device (kW).

The same equations can be used for estimating the time required for the powertrain system to meet the demand required:

$$\frac{P_{FuelCell}}{P_{max}} = \tanh(0.12 * t^{0.8})$$

$$\tanh^{-1}\left(\frac{P_{FuelCell}}{P_{max}}\right) = \frac{3}{25} * t^{\frac{4}{5}}$$

$$\frac{4}{5} \ln(t) = \ln\left(\frac{25}{3} \tanh^{-1}\left(\frac{P_{FuelCell}}{P_{max}}\right)\right)$$

$$t = \left(\frac{25}{3} * \tanh^{-1}\left(\frac{P_{FuelCell}}{P_{max}}\right)\right)^{\frac{5}{4}} \quad (4)$$

Where,  $t$  is the time expected for the fuel cell to reach its maximum power rating, from a given output.

The specific fuel consumption (s.f.c. in g/kWh<sub>e</sub>) for a given power output of the fuel cell system, can be calculated using 4th order power curve fit equation (5)

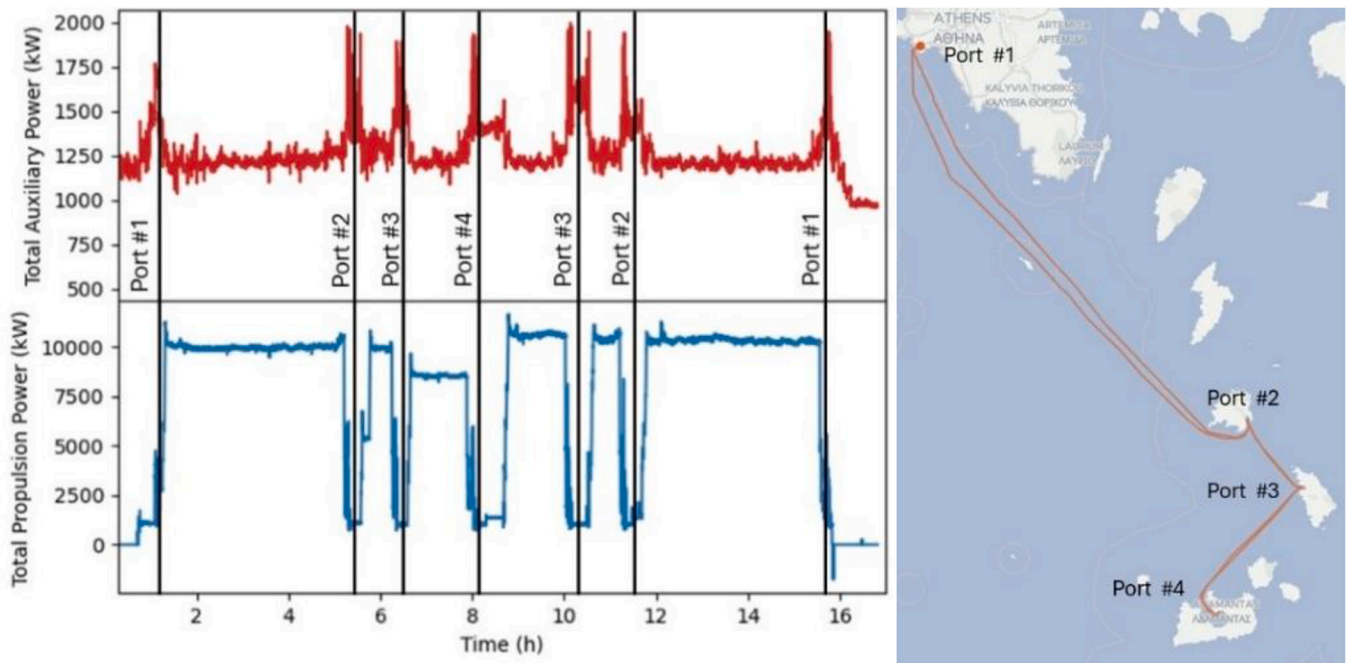


**Fig. 7.** Recorded data of propulsion power demand (blue) along with auxiliary demand (red) for vessel case study examined (left) and travelling route followed (right). Note: Auxiliary demand peaks during each port visit, as indicated by the reduced propulsion demand. This is due to the additional power required to use winches, bow thrusters and equipment for manoeuvring and mooring. Total number of port stops is 5, excluding the final port call, which is the voyage's starting point. Total distance covered for the voyage is 220 nautical miles. (For interpretation of the references to colour in this figure legend, the reader is referred to the Web version of this article.)

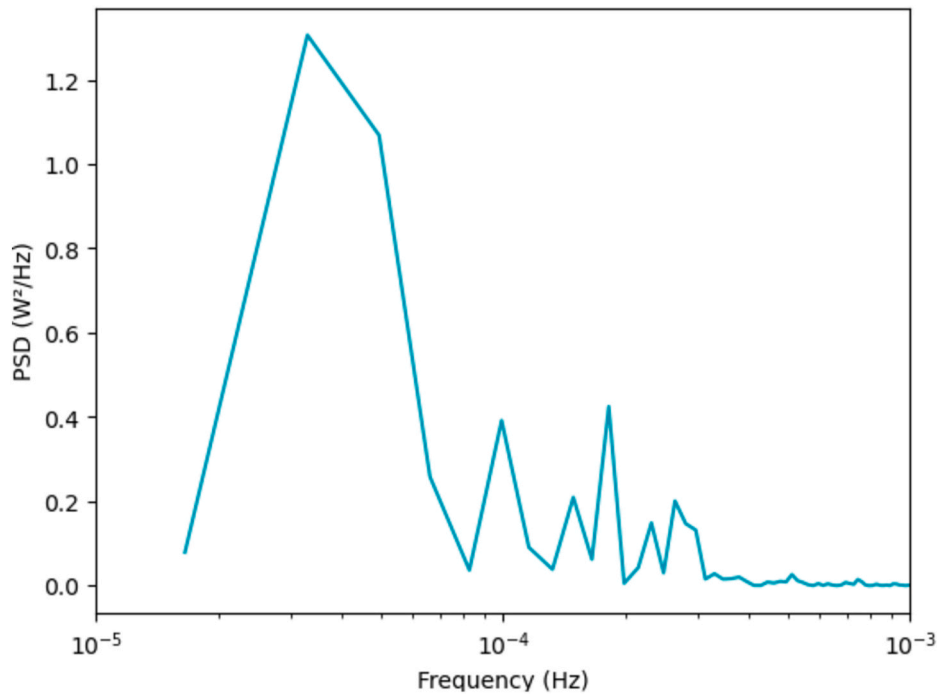


**Fig. 8.** The Power Spectral Density graph for any given frequency is identified in the power demand recordings. The PSD ( $W^2/Hz$ , which is in  $10^6$ ) is a metric that identifies the strength of each signal frequency within the power recordings that are interpreted as the main signal. Anything above 0.03 Hz of relative frequency or a 30 s time period (sampling rate is 1 Hz) is shown to have low relative signal strength and is therefore considered “noise”.

$$s.f.c.PEM = 80 \cdot p^4 - 240 \cdot p^3 + 244 \cdot p^2 - 88.8 \cdot p + 61.943 \quad (5)$$

Where,  $p$  is the loading ratio of the fuel cell units, expressed as a ratio of their instantaneous power output to their maximum rating. A 5 % margin of error is expected on the final consumption values gathered, as

per the IEC 62282 standard (IEC 62282, 2020). A detailed efficiency map with respect to the fuel cell power loading is provided in parallel with equation (5) (Fig. 12).

Since the batteries act like buffers in the current powertrain proposition, the state of charge is set by the following equations:

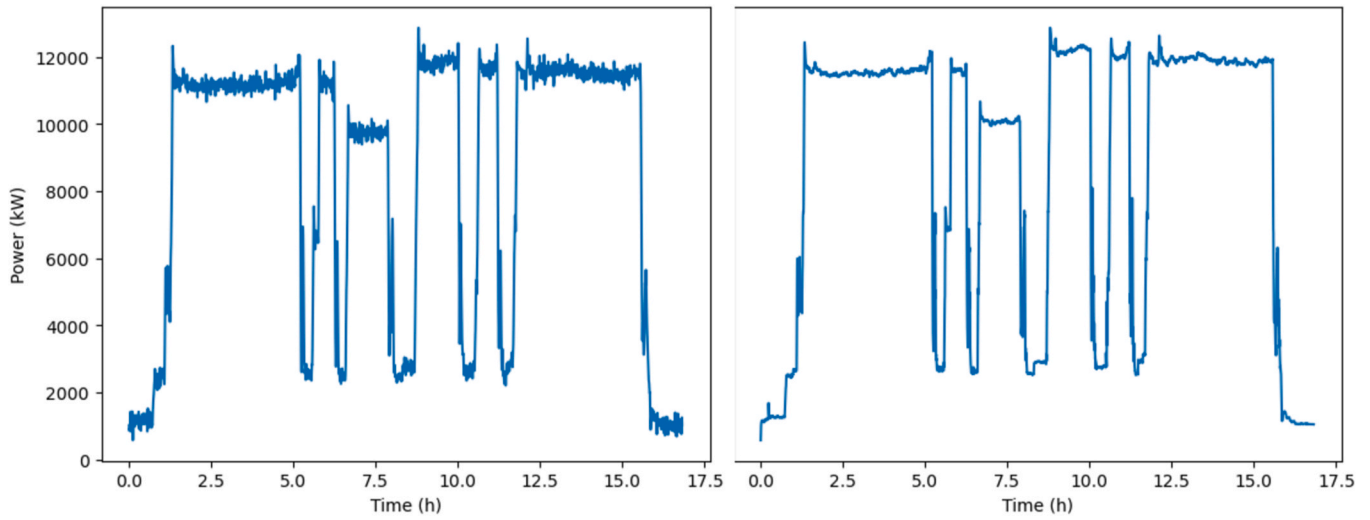


**Fig. 9.** Total power demand recordings for vessel case study examined. The Unfiltered version (left) of the recordings includes noise as expected from electrical components whereas noise is removed from the filtered data (right). Both datasets have the same total electrical demand of 514 GJ. The five drops in power correspond to the intermediate stops where limited propulsive power is required.

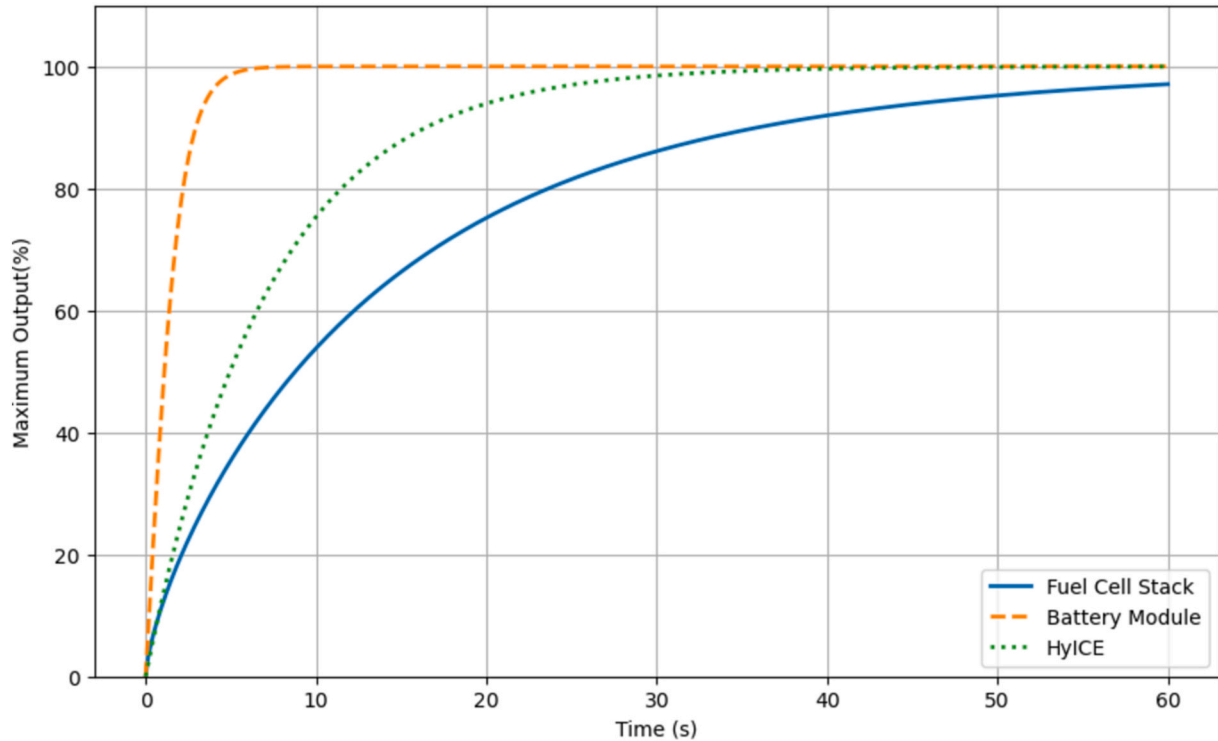


**Fig. 10.** Representation of power ramping rates of the different electricity supplying equipment employed onboard. Batteries provide the most rapid response to demand, whilst fuel cells are the slowest, with HyICE having an intermediate response.

$$P_{\text{Battery}} = P_{\text{tot}} - P_{\text{FuelCell}} \quad (6)$$

$$SoC_1 = SoC_0 - \frac{P_{\text{Bat}} \cdot \delta T}{n} \quad (7)$$

Where,  $P_{\text{tot}}$  is the total power demand on board,  $SoC$  is the batteries' State of Charge and  $\delta T$  is the time passed for a given interval. Each interval is set when the power of the fuel cells exceeds or stands below the power demand of the vessel, until it does not. Finally, the fuel cells are set to dynamically ramp their power output, according to the battery charge level or according to the level of power demand with respect to the fuel cell's minimum and maximum power output. Two separate

simulations were carried out, to investigate how the different fuel cell operational technique influence battery demand.

This is done via *If* loops connected to set operational *response* modes within the python script. One example of such an operational mode is where the fuel cells are set to maximize their power output when the level of battery charge is below 60 %, while the follow-up response mode targets the optimum fuel cell power rating for when the level of charge is above 75 %. Based on the same *If* loop concepts and associated response mode again, fuel cells are set to respond by reducing power output to their minimum when batteries reach 90 % charge.

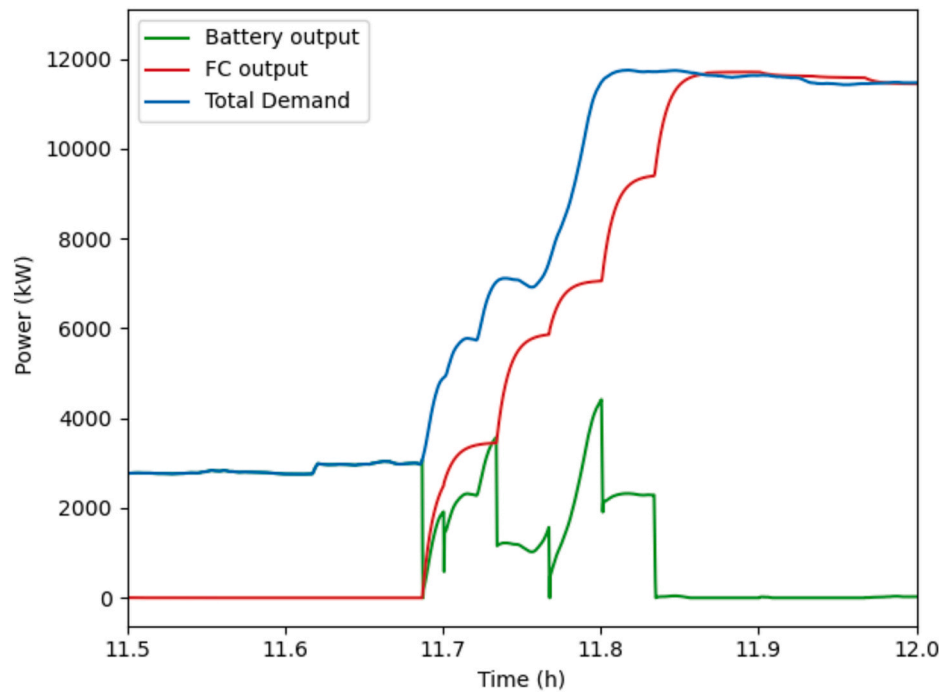


**Fig. 11.** Fuel cell power output (red) responding to the onboard power demand (blue) during a particular time interval of the representative voyage and battery power input required to supply the power deficit (green). Note: Fuel cells show a stepped response to power demand, requiring the batteries to “fill” the power gap. (For interpretation of the references to colour in this figure legend, the reader is referred to the Web version of this article.)

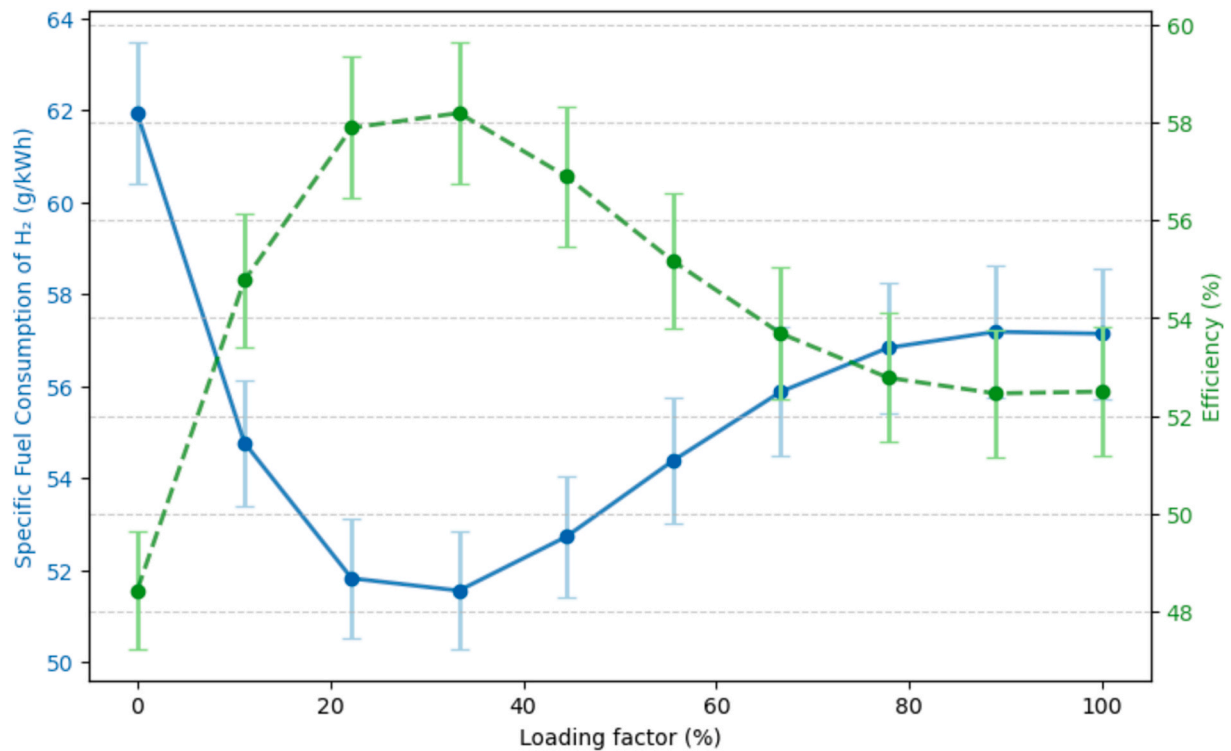


**Fig. 12.** Expected specific fuel consumption of PEM FC stacks and subsequent energy efficiency (Green). The percentage error is expected to be within 5 %, as per IEC 62282 (IEC 62282, 2020). (For interpretation of the references to colour in this figure legend, the reader is referred to the Web version of this article.)

#### 4.4. Hydrogen combustion simulations

There are currently only a few commercial HyICE for marine applications. Most of the examples available follow 4-stroke diesel combustion principles, requiring the use of pilot fuel as an ignition source

(Boretti, 2020/09), similar to methanol and ammonia combustion concepts. This is also done to have a back-up fuelling source onboard, in case there is a lack of hydrogen bunkering infrastructure.

As the purpose of this study is to investigate the viability of implementing HyICE in maritime, results and technical outcomes from other

case studies which focus on the operational characteristics for pre-chamber ignition mechanisms, were used instead. The studies evaluated, use both CFD simulations and experimental data (Gomes Antunes et al., 2009) to assess the combustion characteristics of hydrogen under different injection behaviours and ignition strategies (Boretti and Watson, 2009/03; Boretti et al., 2010b). The efficiency values with respect to the load of a hydrogen combustion engine is subjected to, are taken from the review by Younkins et al. (2013). It is expected that HyICE will undergo a typical four-stroke Otto cycle operation, while using pre-ignition chambers (Boretti, 2020/09) to ignite a inhomogeneous, hydrogen-rich air fuel mixture, with hydrogen being injected as a gas at 200 bar and 300K, which then ignites a secondary, lean-hydrogen fuel air mixture within the main combustion chamber (Boretti et al., 2010a; White et al., 2006/08). Once again, it is assumed that LH<sub>2</sub> boil-off gas is used as the immediate fuel supply, with its gasification and pressurisation having no effect on the overall energy demand of the vessel. Examples of such combustion technology are already being used for motorsports (Boretti, 2019/03) and available from established engine manufacturers (Mahle Powertrains). Fig. 13 shows the expected efficiency of the engine for the subsequent load. It is important to note how major maritime engine manufacturers state ~50 % generator efficiencies for current products on the market, which use gaseous fuels and combust under Four-Stroke-Otto cycle principles ("WÄRTSILÄ 31SG, 2023).

As observed, total thermal efficiency is expected to be reduced when reducing the load, as is typical with ICE gensets. Peak operational efficiency is expected to be reached at 80 % of the maximum load rating (Fig. 13), even though efficiency can further increase, as this is recommended to be a safe operational mode for the engine ("WÄRTSILÄ 31SG, 2023). To include this in the python code, additional equations and *if* loops linked to new response modes, were developed, as shown in equations 8–11. What differs for the sole HyICE and battery powertrain scenario, is the exclusion of the fuel cell power output and the inclusion of four generators (Table 1), where the number of generators that are activated at any given point in time, is determined by the power demand experienced onboard and the batteries' state of charge.

While equations (1)–(7) are still included inside the code, a new parameter is introduced regarding load prioritisation, as shown in equation (9).

$$P_{Demand} = P_{tot} - P_{FuelCell} \quad (8)$$

Through the implementation of *if* loops, when the demand is lower than half of the generator's maximum power output, then it is met through batteries, as shown in equations (5) and (6). If, however, either the batteries' level of charge is less than half of their maximum level and the demand is less than or equal to the generator's optimum power output, then:

$$P_{Demand} = P_{HyICE} \quad (9)$$

Time is required for HyICE to reach their demand as shown in equation (10), while the fuel consumption (in g/kWh) of the engines is determined using equation (11), including a 5 % error (ISO 3046, 2002).

$$t_{ICE} = \frac{P_{HyICE}}{0.025} \quad (10)$$

$$s.f.c._{HyICE} = 24.29 * p^2 - 47.08 * p + 82.317 \quad (11)$$

For these simulations, it is assumed that typically 10 s are required for the generator to start producing energy at the rated loading (Equation (10)), assuming that engines are already started-up, pre-lubricated and warmed up. The entire start-up procedure could take up to 60 s (Wärtsilä 25DF Product Guide) and is therefore compensated within the code by taking into account the vessel's speed, which indicates the vessel's switch in operational profiling (e.g., from sailing to port approach) as well as the batteries' state of charge relative to the fuel cell's power output.

An additional stand-by mode is also considered for when the vessel is between operational profile switches, or when the fuel cells are providing minimum power output. This mode considers the HyICE as operating and therefore consuming energy yet not connected to the local grid. In both scenarios the total consumption occurring as a result of the start-up and stand-by procedures, is included in the final consumption

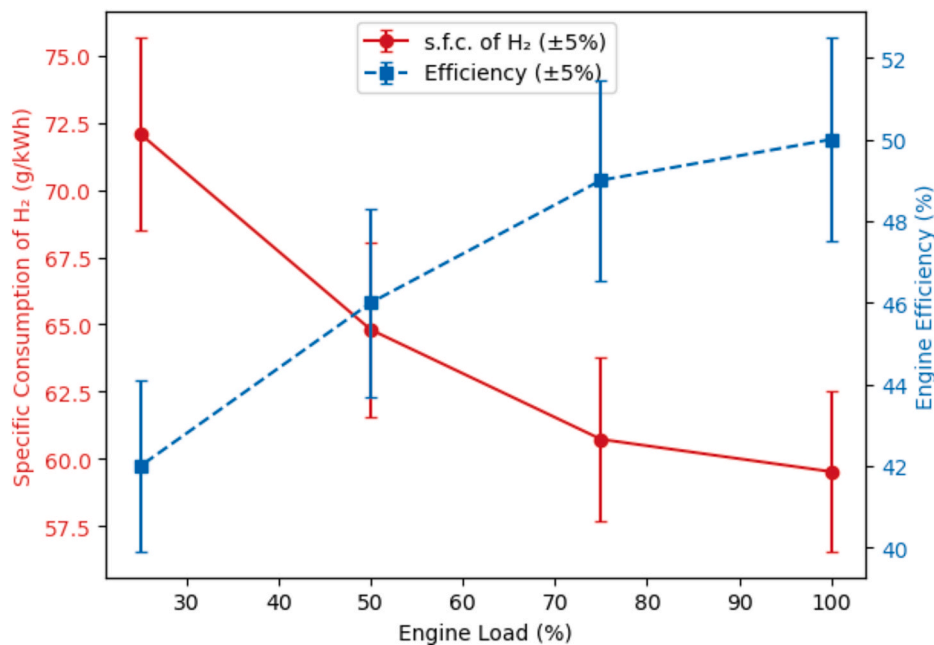


**Fig. 13.** Expected (Boretti, 2020/09) specific fuel consumption of 4-Stroke Otto hydrogen combustion engine model (red) and subsequent energy efficiency (blue). Note: Electricity conversion losses are expected from running ICE as gensets (3 %), with literature review indicating a HyICE efficiency of ~50 % (Boretti, 2020/09), therefore a total generator system peak efficiency of 50 % was assumed. This is below the value claimed by current industry product examples ("WÄRTSILÄ 31SG, 2023). The percentage error is expected to be within 5 %, as per ISO 3046 (ISO 3046, 2002). (For interpretation of the references to colour in this figure legend, the reader is referred to the Web version of this article.)

figures gathered, assuming that engine starting occurs with stored, compressed air and has negligible parasitic losses on the rest of the system. When introducing an auxiliary power output such as ICE, the battery capacity required is expected to be significantly reduced, provided that the gensets make up the lost percentage of electrical power output.

## 5. Results

### 5.1. Scenario 0: original vessel powertrain

The simulated fuel consumption values result from the onboard power recordings gathered, along with the manufacturer's operational profiles for the diesel engines employed onboard, with the subsequent emissions estimated based on typically accepted factors presented as mass per energy of fuel consumed (I.M.O., 2023; Ekmekçioğlu et al., 2020/11). The calculated voyage consumption was 5.1 t and 25.0 t of diesel for the auxiliary and propulsion engines respectively, resulting in a total fuel energy consumption of 1,285 GJ. The operators bunker the vessel every three days and confirmed a total amount of 90 tonnes being bunkered ( $\pm 0.5$  tonnes), yielding an average daily MGO consumption of 30 tonnes ( $\pm 0.2$  tonnes), an amount that it is within the margin of error (within 1 %) of the value calculated here from our time-domain based simulation. The estimated resulting emissions from a representative voyage are 94.5 t of CO<sub>2</sub>, 280 kg of SO<sub>x</sub>, 1.9 t of NO<sub>x</sub> and 400 kg of PM. These results provide a baseline for comparison in the rest of this study. By considering the total fuel energy consumed and the total energy demand based on the vessel's recordings, the overall tank to propeller efficiency is calculated to be 39 % ( $\pm 2$  %).

### 5.2. Scenario 1: HyICE powertrain

Our first scenario assumes that the vessel is converted to a hydrogen-ICE electric powertrain, without the option of battery energy storage. Using the four stroke Otto spark ignition principles examined in Section 3, our calculations indicate that hydrogen combustion can improve the vessel's overall efficiency. This first iteration of the HyICE powertrain was assumed to directly substitute the equipment that is already in place, without any further optimization. This scenario is deemed unrealistic due to the lack of optimization, because the main engines run on average at 50 % loading because of the targeted speeds recorded. Regardless, the vessel's final efficiency was increased to  $44 \pm 2.3$  %.

which is a  $\sim 5$  % increase in efficiency, with a total fuel consumption of  $9,346 \pm 467$  kg LH<sub>2</sub>. Although the efficiency improvement is minor, HyICE have the potential to boost the total fuel efficiency of the vessel under the operational conditions considered.

### 5.3. Scenario 2: HyICE and battery powertrain

Our second scenario introduces a battery to the HyICE powertrain, similar to that for the fuel cell powertrain arrangement, and provides a more direct method of comparison between the two primary hydrogen electric powertrains proposed in this study. Four 4.5 MWe generators were selected to achieve this, along with 2.5 MWh battery storage, based upon the total propulsion power already installed and the expected auxiliary demand (2.5 MW). Fig. 14 shows how the HyICE electric powertrain responds to the loads it is subjected to during the voyage.

The total consumption of the vessel with the HyICE genset and battery powertrain was estimated to be  $8,661 \pm 433$  kg of LH<sub>2</sub>, yielding a total efficiency of 49 % ( $\pm 2.5$  %) when accounting for the net change in battery state of charge (2,250 MWh). This is due to the operational mode set for the internal combustion engines, enabling a specific 80 % loading factor, yielding the highest possible efficiency without exceeding the maximum output rating. At the same time, excess energy is used to charge the batteries which, similarly to FC powertrain propositions, means that they serve as a buffer for the total vessel demand. Their maximum discharge rate is limited at a momentary 3C or 7.5MWe (Ning et al., 2003/05; Vega-Garita et al., 2024), and as shown in Fig. 14, this is not exceeded at any given point in the vessel's voyage.

### 5.4. Scenario 3: H<sub>2</sub> fuel cell electric powertrain

Fuel cells will have different responses to the power demand of the vessel compared to an ICE. Despite the different control methods employed to alter their power output, the batteries employed onboard, act as electrical power buffers. This can be achieved via the implementation of a low-pass filter, the limiting frequency of which is not known until Fast Fourier Transforms (FFT) are used to identify the dominant signal frequencies. Fig. 9 shows the comparison between the original power data and its filtered version which is meant to replicate the battery reaction to the load it is subjected to. Both filtered and unfiltered version of the data set recorded, show the same energy demand.

Using the filtered version of the power demand data, the fuel cell

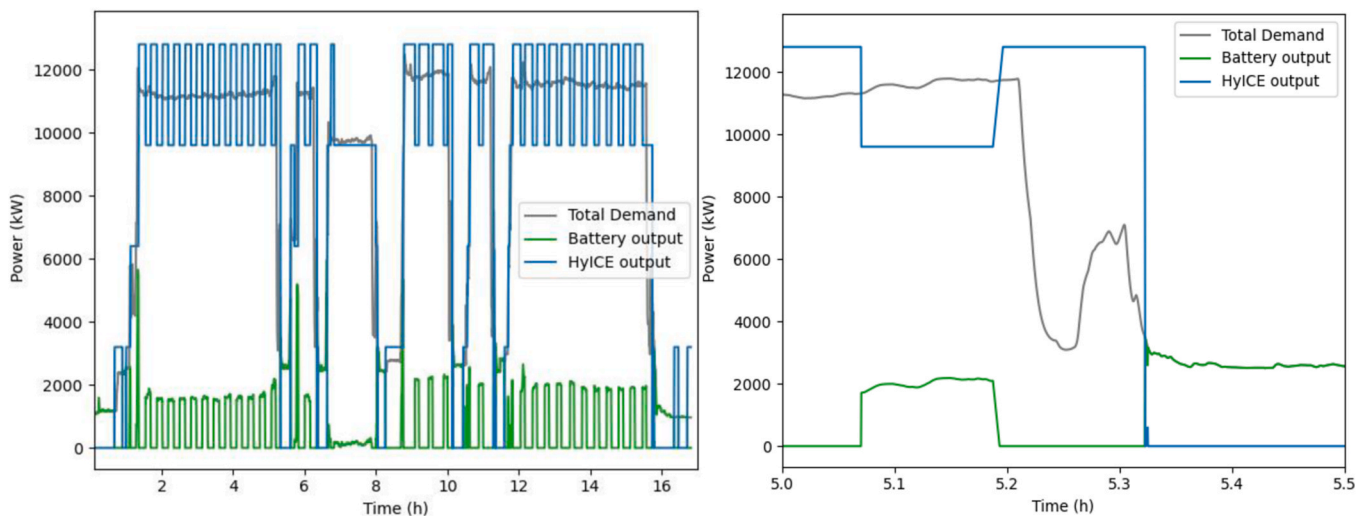


Fig. 14. HyICE gensets and battery powertrain proposal (Scenario 2). Note: All four HyICE gensets are set to run at 80 % loading when required. Note: To maximize efficiency, the gensets are only set to run at 80 % factor, whilst maintaining a certain level of charge for the batteries. When the level of charge is satisfactory, batteries are used in favour of at least one generator, as shown in a particular point in time (right).

simulation code was employed with two different modes of operation; one that focuses on keeping the fuel cells at a steady operational level and the other focusing on reducing the required battery size by following the load dynamically (Fig. 15).

Final battery sizing was selected based on the total auxiliary demand expected (2.5 MW), which is the maximum peak in demand expected at any given point in time. This would require a maximum spontaneous discharge power of 3C, or approximately 7.5 MWe (Ning et al., 2003/05; Vega-Garita et al., 2024) for the battery pack selected. This will be necessary, as shown in Fig. 11, due to the expected rapid power requirements being greater than 5 MW. Even when using the dynamic load following condition that has a lower battery demand, the response of the PEM FCs remains a limiting factor due to their inability to increase their power output at the same rate as an ICE. This is illustrated with greater detail in Figs. 10 and 11.

The final consumption for this scenario 3 is 7,893 kg of LH<sub>2</sub> ( $\pm 395$  kg LH<sub>2</sub>), indicating a total efficiency of 54 % ( $\pm 2.7$  %). This is a  $\sim 10$  % improvement over the original diesel powertrain, whilst utilising a zero-emission fuel. However, the same cannot be said for the HyICE genset and battery powertrain (Scenario 2), where final efficiency is almost 49 % ( $\pm 2.5$  %), raising the question whether combining the three different powertrains would improve total vessel efficiency or not.

#### 5.5. Scenario 4: Fuel Cell and HyICE electric powertrain (Triple hybrid)

A major aim of this study is to investigate whether traditional technologies can assist the rapid transition to low carbon shipping, in similar ways to previous transitions, through the combination of new concepts with existing propulsion powertrains. To optimise this approach, we tailor the size of individual powertrain components to the vessel's energy needs, with the ideal combination providing the lowest consumption for the lowest battery power demand. Fig. 16 is used to show how the ideal combination of HyICE and battery sizing was selected, through testing different sizes for both.

Based on Fig. 16, the best combination is a 700kWh battery with a 2.0 MWe HyICE generator. The final consumption increased by 0.4 % or to 7,938 of kg LH<sub>2</sub> ( $\pm 397$  kg LH<sub>2</sub>) which is well within the margin of error. This shows how improving the system redundancy yields a similar overall efficiency, while reducing the original battery capacity by 72 %, as the peak battery demand is significantly reduced ( $-55$  %) due to the

presence of the HyICE generator.

The results of this case study are further illustrated in Fig. 17, where the peak power demand required from the batteries is significantly reduced by introducing the HyICE generators, allowing the expected power demand to be met whilst leaving the total efficiency relatively unchanged.

### 6. Multi criteria assessment of powertrain scenarios

Fig. 18 shows the estimated mass and volume comparison for the individual components of each system examined in this study, as well as their installation costs based on values from Table 4 which indicates relevant source.

Fig. 18 illustrates how HyICE with batteries (Scenario 2) can significantly reduce machinery space and weight over FCs with batteries for the utilisation of LH<sub>2</sub>, even though there is an efficiency disadvantage of  $\sim 5$  %.

Table 5 summarises the efficiency and consumption results for all scenarios. It should be noted that final vessel GHG emissions are expected to be eliminated, since the exhaust gases will be water vapour from either the HyICE or FC.

A judgement is required as to whether the space saved, is more important to stakeholders than the increase in fuel consumption, which is 5 % higher than Scenario 3. This judgement will by necessity depend on the duty cycle and type of the ship. From a total cost of ownership perspective, it is worth pointing out that break-even point between conventional diesel electric and HyICE powertrain could be reached before the vessel's end of life, assuming similar maintenance costs, fuel price is a current value for diesel and actual Liquid Hydrogen costs were 3.5 times current diesel prices, from a \$/GJ perspective, as every hydrogen powertrain examined would be more efficient, therefore saving on fuel cost. However, the total amount of time required to reach this break-even point, would also depend on any emission penalties imposed and the frequency of voyages. A significant reduction of capital expenditure is also expected for the HyICE and batteries powertrain. The onboard machinery space requirements of the HyICE-battery combination is only slightly greater than existing diesel powertrain demands, but significantly lower ( $<40$  %) than other arrangements requiring large battery packs. Consequently, HyICE-battery hybrids may be a more suitable powertrain approach for high power density vessels, despite the

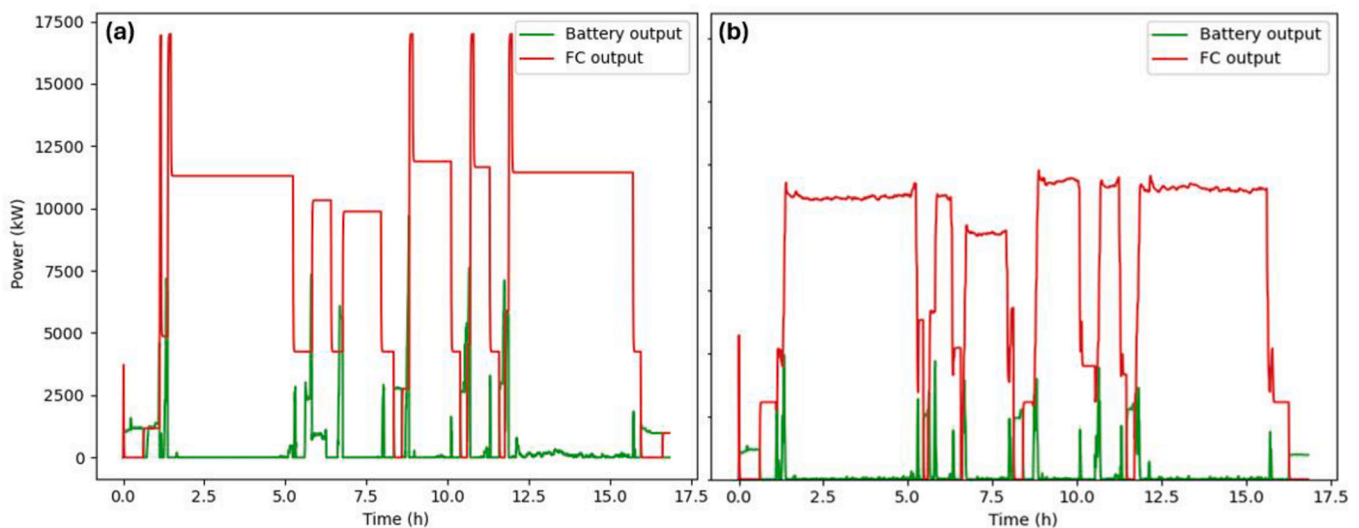
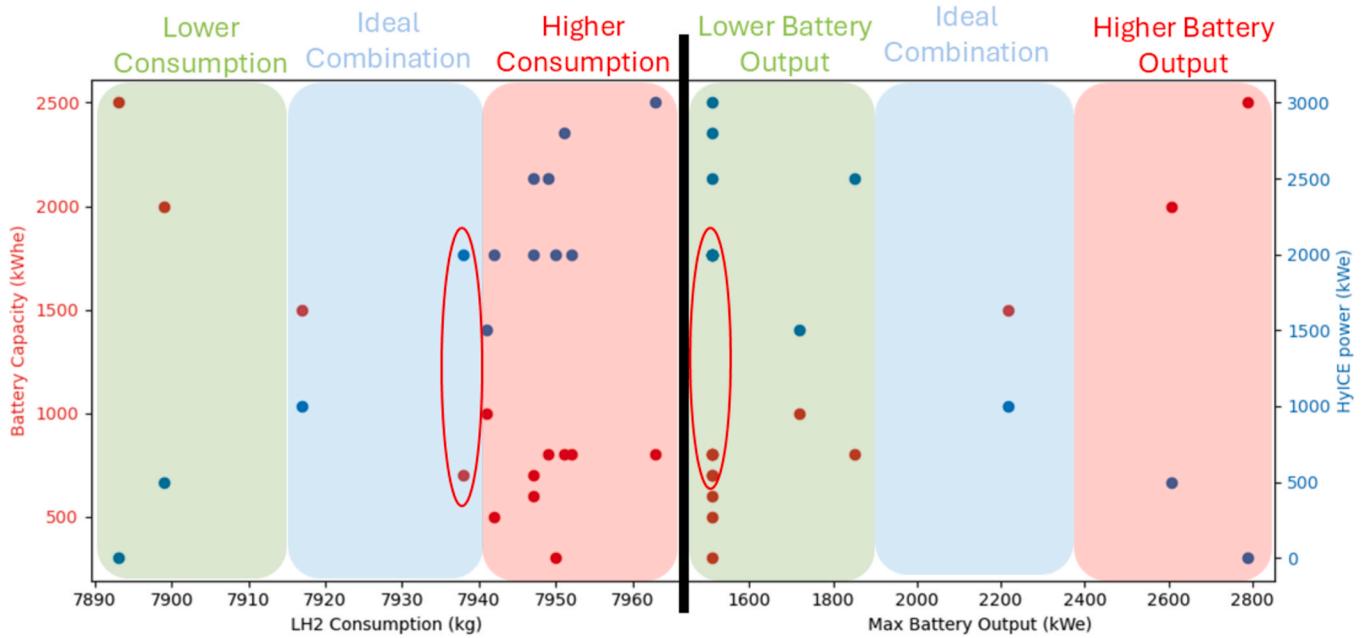
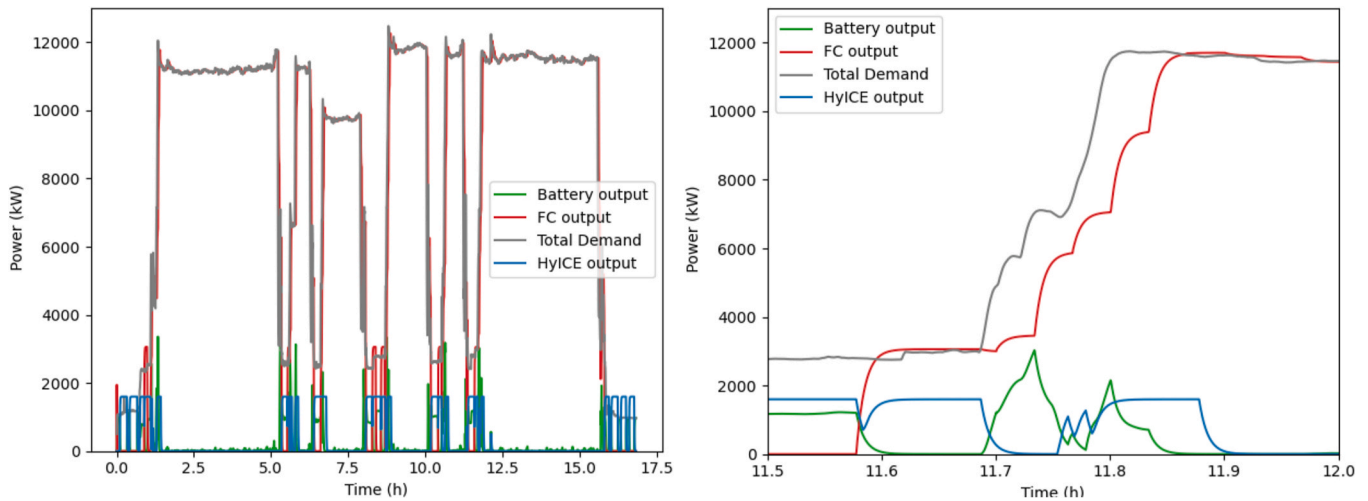


Fig. 15. Battery demand for steady state operation of fuel cells (a) against the dynamic load following behaviour proposed (b). Power peaks result from battery charge levels falling below their state of charge safety margin. It is also clear how during port calls, fuel cells shut down to conserve energy, requiring the batteries to serve as the main power source. However, when propulsion demand spikes, the fuel cells' power ramping rate is too slow and overtaken by the demand, requiring the use of batteries. When running at a steady state mode (a), the demand on batteries is higher (9.7MWe) and requires greater battery capacity than is required in a dynamic load following mode (b) (7.5MWe).



**Fig. 16.** Fuel consumption (left) resulting from expected maximum Battery output (right), depending on Battery capacity and Internal Combustion Engine power output selected. Note: Each dot represents a different simulation result. Fuel cell installed power output remains at 17 MW, as with the FC-battery powertrain simulation for direct comparison. The purpose of this figure is to select the HyICE power output (Blue Dots) to minimise battery capacity demand (Red Dots) on board, allowing the installation of smaller batteries, whilst lowering the total powertrain consumption, with the ideal combination indicated (Red oval). (For interpretation of the references to colour in this figure legend, the reader is referred to the Web version of this article.)



**Fig. 17.** Response of the three different powertrain systems over the entire trip (left) and for a selected time interval whilst leaving port 11.7 h into the voyage's duration (right) Note: HyICE are used as an intermediate buffer between the vessel's demand and the fuel cells instead of batteries. When in port or during periods of low demand, HyICE are employed instead of fuel cells.

minor (~5 %) increase in hydrogen fuel demand.

All considered, the purpose of this study is not to complete a full technoeconomic assessment of each powertrain scenario examined here. Instead, the purpose is to calculate the installation costs of each equipment and compare it to the final calculated efficiency values. Further work is required for a complete technoeconomic assessment, which is outside the scope of this study.

## 7. Study assumptions and limitations

The purpose of this study is to examine and compare potential hydrogen fuelled powertrains in terms of overall energy efficiency, space, weight and installation costs. The results presented come from

assumptions made regarding the fuel supply system, as well as a standard percentage of error for most values presented, relevant to efficiency and consumption of the powertrain equipment. This percentage of error is in line with international standards, meant to take into account environmental conditions and calculation/recording instrument errors.

The powertrain simulation model discussed in this study, is considered as a simple yet replicable tool for individuals to reproduce the results presented here or to investigate concept applications in other vessels. Although other simulation tools are available in the market, to the Authors' knowledge, such software is yet to be validated against vessels with modern powertrains, while it also provides similar powertrain efficiencies and response values to the ones' presented in this study (Bassam et al., 2017/01), depending on the set-up. Moreover, this study

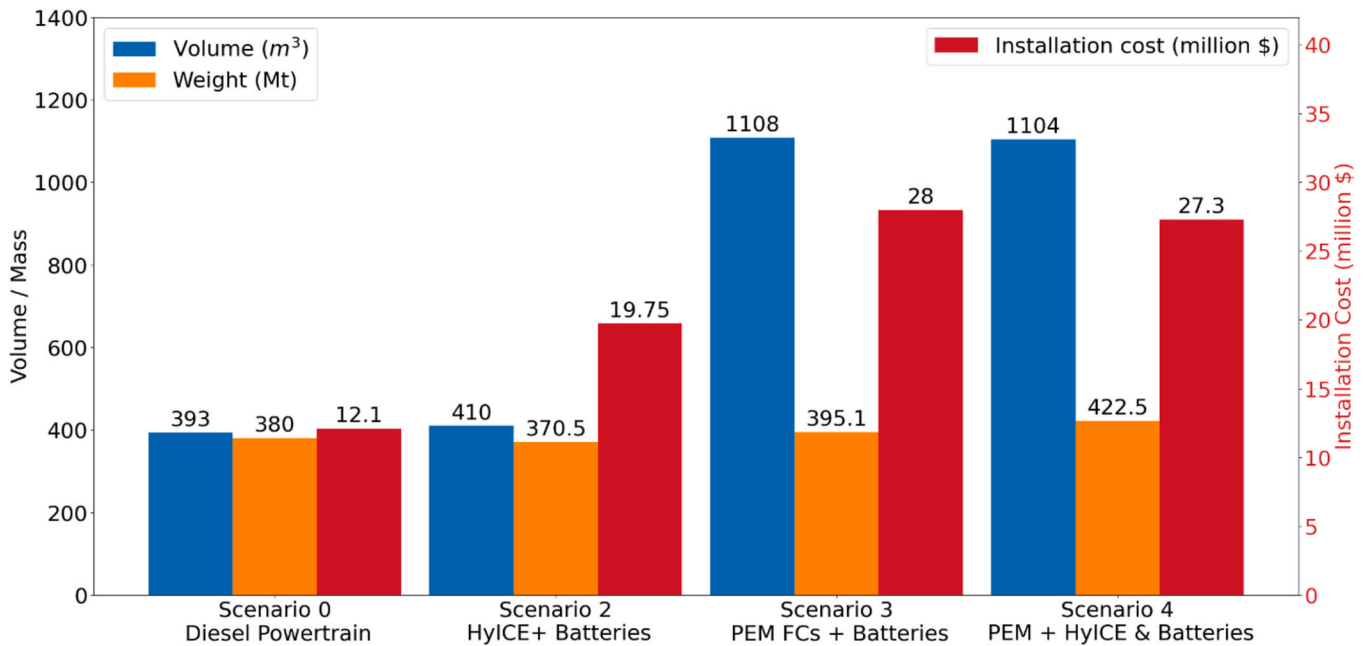


**Fig. 18.** Total equipment size and volume for each powertrain case study examined (Table 4 for details). The hydrogen generator and battery powertrain (Scenario 2) provides the lowest occupation by volume in terms of total machinery space, yet this comes with an efficiency loss of 5 % compared to the other powertrain case studies examined. Scenario 1 is omitted since it is Scenario 2 without the inclusion of batteries.

**Table 4**

Key properties used for space weight and cost estimation for individual equipment.

Equipment	Cost (\$)	Volume (m <sup>3</sup> )	Mass (Mt)
Batteries (per kWh)	700 (Mauler et al., 2021)	0.02 (Kaur et al., 2022)	0.033 (Kaur et al., 2022)
Fuel Cells (per kW <sub>e</sub> )	1500 (Fu et al., 2023)	0.062 (PemGen MT)	0.02 (PemGen MT)
Gensets (per kW <sub>e</sub> )	1000 (Ritari et al., 2023)	0.02 (Wärtsilä 31SG, 2023)	0.016 (Wärtsilä 31SG, 2023)
Diesel ICE propulsion system (per kW)	600 (Baldi et al., 2019)	0.019 (S.E.M.T. PIELSTICK, 1995)	0.019 (S.E.M.T. PIELSTICK, 1995)

**Table 5**

Powertrain configurations examined and final results.

Scenario	Powertrain Type	Powertrain Specifications	Total Efficiency and Fuel Consumption
1	HylCE Gensets	4x Hydrogen Combustion Generators (18 MWe)	44 ± 2.3 % 9,346 ± 467 kg of LH <sub>2</sub>
2	HylCE Gensets&Batteries	4x Hydrogen Combustion Generators (18 MWe) Marine battery pack 2.5 MWh	49 % (±2.5 %) 8,661 kg of LH <sub>2</sub> (±433 kg LH <sub>2</sub> )
3	PEM Fuel Cells&Batteries	30x Hydrogen PEM Fuel cell stacks (18 MWe) Marine battery pack 2.5 MWh	>54 % (±2.7 %) 7,893 kg of LH <sub>2</sub> (±395 kg LH <sub>2</sub> )
4	PEM Fuel Cells with HylCE Gensets& Batteries	30x Hydrogen PEM Fuel cell stacks (18 MWe) 2.0 MWe HylCE Genset Marine battery pack 700 kWh	<54 % (±2.7 %) 7,938 kg of LH <sub>2</sub> (±397 kg LH <sub>2</sub> )

is considered as a systems-level approach with an emphasis on assessing system deployment feasibility, not for energy management system optimization. An effort is made for benchmarking the operational

simulation model presented here with the current powertrain of the vessel, yet the same cannot be done for the FC hybrid model. Also important to note is the attempt for matching the hybrid powertrain response to that of a Diesel-ICE one. In reality, this might not be necessary with slower response rates still being acceptable, yet to an unspecified extent.

Part of the narrative behind hydrogen utilisation as a fuel is to reduce emissions from a Lifecycle assessment perspective. The use of “green” hydrogen would be ideal with an embedded carbon footprint anywhere between 5 and 15g of CO<sub>2</sub>equiv/MJ (Thomas, 2018) of fuel consumed significantly lower (+80 %) than that of diesel at 90g of CO<sub>2</sub>equiv/MJ of fuel consumed (Edwards et al., 2014), however, other hydrogen types resulting from fossil fuel reforming could be worse than current diesel alternatives (Busch et al., 2023/09). A holistic lifecycle assessment of the fuel and powertrain employed on this vessel throughout its lifetime is required to provide final emission saving values, switching from a diesel-ICE powertrain to an FC hybrid fuelled via green hydrogen. Finally, a technoeconomic assessment of the powertrain hybrids presented here would be ideal, yet this would necessitate the deployment of a separate study.

## 8. Conclusion

With the urgent need for shipping to decarbonise by 2050, a range of alternative fuels and powertrains have been suggested but to date there is no consensus. This is impeding the adoption of potential low-carbon power concepts. However, this is not the first major maritime transition, and past behaviours indicate that the likely approach through which shipping will achieve a rapid green transition is through the partial utilisation of well understood existing technology for which industry has great experience.

A time domain based, bottom-up simulation of powertrain operation was developed to examine the different powertrain combinations. The model was benchmarked against data from the representative ship with a voyage fuel consumption error of order 1 %, yet further validation is required regarding the FC hybrid powertrains examined.

All LH<sub>2</sub> fuelled powertrains could yield significant CO<sub>2</sub>equiv reductions (−80 % if green hydrogen is selected), with the final carbon

footprint of the vessel case study, being directly proportional to the embedded carbon footprint per unit of hydrogen mass produced. Although green hydrogen would ultimately be preferred, this is not the only option currently available. Further work is required from a lifecycle assessment perspective on the powertrain hybrids discussed, to provide final emissions savings compared to the current powertrain.

Regardless, it is shown that for a high energy demand ship undertaking a short voyage with regular port calls, a low-carbon HyICE genset and battery powertrain has 6 % greater total energy efficiency when compared to conventional diesel powertrains and is only 5 % less efficient in terms of Liquid H<sub>2</sub> fuel consumed than a hydrogen fuel cell and battery system, indicating that pre-existing powertrain technologies can be used with new fuels.

The space and cost demand of the HyICE-battery system are 70 and 30 % lower respectively compared to a hydrogen fuel cell installation cost. For the vessel considered, the space-saved by the HyICE-battery powertrain could provide additional fuel storage to increase its operational range. Further work is encouraged on examining the long-term impacts of each powertrain proposed, from a cost benefit perspective. It is expected that hydrogen powertrains will be a more cost-effective option compared to diesel ones, in the long term, with the cost benefit being dependent on external factors such as emission penalties imposed, yet a separate and dedicated technoeconomic study is required to confirm this.

A combination of both HyICE and FCs is examined in this paper indicating that efficiency, space and weight occupation, are similar. This makes an excellent case of including added power redundancy on board future ships, whilst allowing the crew to become more familiar with the new-to-them fuel cell technology. From evaluating the different powertrain scenarios, it is expected that final triple hybrid powertrain efficiencies will vary proportionally to the percentage of power contribution from HyICE or FCs.

#### CRedit authorship contribution statement

**Panos Manias:** Writing – original draft, Visualization, Validation, Software, Resources, Methodology, Investigation, Formal analysis, Data curation, Conceptualization. **Damon A.H. Teagle:** Writing – review & editing, Writing – original draft, Supervision, Project administration, Funding acquisition. **Dominic Hudson:** Writing – review & editing, Supervision. **Stephen Turnock:** Writing – review & editing, Writing – original draft, Resources, Project administration, Funding acquisition.

#### Declaration of competing interest

The authors declare the following financial interests/personal relationships which may be considered as potential competing interests: Panos Manias reports financial support was provided by University of Southampton. Panos Manias reports financial support was provided by Horizon Europe. Panos Manias reports financial support was provided by Shell International Trading and Shipping Company Limited. The corresponding author is completing a Part-Time PhD, funded by the University of Southampton's Maritime Engineering department and by an industrial sponsor: Shell International Trading and Shipping Company Limited. His Full-Time researcher role for the Southampton Marine and Maritime Institute, is supported by the EU Horizon's Maritex-X innovation funding. If there are other authors, they declare that they have no known competing financial interests or personal relationships that could have appeared to influence the work reported in this paper.

#### Acknowledgements

This paper is the result developments enabled through projects completed under the Innovate UK Clean Maritime Demonstration Competition. The authors are also grateful for the financial support provided via the EU Horizon 2020 Maritex-X Teaming project (EU

H2020 857586) and the Southampton Marine and Maritime Institute, to Shell Shipping and Maritime for their support of the Centre for Maritime Futures at the University of Southampton and to Aegean Sea Lines for kind provision of real high frequency energy demands for the M/V Anemos.

#### Nomenclature:

NH <sub>3</sub>	Ammonia
DAC	Direct Air Capturing
CCU	Carbon Capture and Utilisation
CO <sub>2</sub>	Carbon Dioxide
FC	Fuel Cell
GHG	Greenhouse Gas
HyICE	Hydrogen Internal Combustion Engine
ICE	Internal Combustion Engine
IMO	International Maritime Organisation
LH <sub>2</sub>	Liquid Hydrogen
LCV	Lower Calorific Value
CH <sub>3</sub> OH	Methanol
NO <sub>x</sub>	Nitrogen Oxides
PEM	Proton Exchange Membrane (fuel cell)
PM	Particulate Matter
SFC	Specific Fuel Consumption
SOFC	Solid Oxide Fuel Cell
SO <sub>x</sub>	Sulphur Oxides

#### References

- Ambient (outdoor) air pollution." World Health Organisation. [https://www.who.int/news-room/fact-sheets/detail/ambient-\(outdoor\)-air-quality-and-health](https://www.who.int/news-room/fact-sheets/detail/ambient-(outdoor)-air-quality-and-health) (accessed December 5th, 2023).
- Ammonia as a Marine Fuel, 2020. DNV GL, Group Technology & Research. Analysing the possibilities of using fuel cells in ships. *Int. J. Hydrogen Energy*, 2016 2853–2866.
- Engine RETROFIT REPORT 2023: applying alternative fuels to existing ships. In: Marine Energy Transition, 2023. Lloyd's Register [Online]. Available: [https://www.lr.org/en/knowledge/research-reports/applying-alternative-fuels-to-existing-ships/?create=676223420777&keyword=methanol%20engine%20retrofit&matchtype=b&network=g&device=c&utm\\_source=google&utm\\_campaign=&utm\\_medium=cpc&utm\\_content=&utm\\_term=methanol%20engine%20retrofit](https://www.lr.org/en/knowledge/research-reports/applying-alternative-fuels-to-existing-ships/?create=676223420777&keyword=methanol%20engine%20retrofit&matchtype=b&network=g&device=c&utm_source=google&utm_campaign=&utm_medium=cpc&utm_content=&utm_term=methanol%20engine%20retrofit).
- Fuel cells for shipping: to meet on board demand and reduce emissions. In: *Energy Reports*, vol. 7, 2021. Elsevier, pp. 63–70.
- Methanol as an alternative fuel for container vessels ". [Online]. Available: <https://www.dnv.com/expert-story/maritime-impact/methanol-as-an-alternative-fuel-for-container-vessels.html>.
- Methanol for the maritime energy transition [Online]. Available: <https://www.man-es.com/marine/strategic-expertise/future-fuels/methanol>.
- Wärtsilä 31SG. In: WÄRTSILÄ 31SG - Product Guide, 2023. WÄRTSILÄ®.
- Al Din Al Hajjaji, S., 2023. National legal models to regulate scrubbers washwater. *Loy. LA Int'l & Comp. L. Rev.* 46, 87.
- Alderman, J.A., 2005. Introduction to LNG safety. *Process Saf. Prog.* 24 (3), 144–151.
- Anicic, B., Trop, P., Goricanec, D., 2014. Comparison between two methods of methanol production from carbon dioxide. *Energy* 77, 279–289.
- Aziz, M., Wijayanta, A.T., Nandiyanto, A.B.D., 2020. Ammonia as effective hydrogen storage: a review on production, storage and utilization. *Energies* 13 (12), 3062.
- Baldi, F., Brynolf, S., Maréchal, F., 2019. The Cost of Innovative and Sustainable Future Ship Energy Systems," *Ecos*, pp. 239–250.
- Bassam, A.M., Phillips, A.B., Turnock, S.R., Wilson, P.A., 2017. Development of a multi-scheme energy management strategy for a hybrid fuel cell driven passenger ship. *Int. J. Hydrogen Energy* 42 (1), 623–635. <https://doi.org/10.1016/j.ijhydene.2016.08.209>.
- Baykara, S.Z., 2018. Hydrogen: a brief overview on its sources, production and environmental impact. *Int. J. Hydrogen Energy* 43, 10605–10614. <https://doi.org/10.1016/j.ijhydene.2018.02.022> [Online]. Available:
- Bayramoglu, K., Yilmaz, S., Nuran, M., 2024. Reduction of the harmful NO<sub>x</sub> pollutants emitted from the ship engines using high-pressure selective catalytic reduction system. *Environ. Sci. Pollut. Control Ser.* 31 (22), 32813–32825. <https://doi.org/10.1007/s11356-024-33439-y>.
- Bhattacharyya, D., Rengaswamy, R., 2009. A review of solid oxide fuel cell (SOFC) dynamic models. *Ind. Eng. Chem. Res.* 48 (13), 6068–6086. <https://doi.org/10.1021/ie801664j>.
- Boretti, A., 2019. Transient positive ignition engines have now surpassed the 50% fuel conversion efficiency barrier. *Int. J. Hydrogen Energy* 44 (14), 7051–7052. <https://doi.org/10.1016/j.ijhydene.2019.01.237>.
- Boretti, A., 2020. Hydrogen internal combustion engines to 2030. *Int. J. Hydrogen Energy* 45 (43), 23692–23703. <https://doi.org/10.1016/j.ijhydene.2020.06.022>.

- Boretta, A.A., Watson, H.C., 2009. Enhanced combustion by jet ignition in a turbocharged cryogenic port fuel injected hydrogen engine. *Int. J. Hydrogen Energy* 34 (5), 2511–2516. <https://doi.org/10.1016/j.ijhydene.2008.12.089>.
- Boretta, A., Paudel, R., Tempia, A., 2010a. Experimental and computational analysis of the combustion evolution in direct-injection spark-controlled jet ignition engines fuelled with gaseous fuels. *Proc. Inst. Mech. Eng. - Part D J. Automob. Eng.* 224 (9), 1241–1261. <https://doi.org/10.1243/09544070jauto1465>.
- Boretta, A., Watson, H., Tempia, A., 2010b. Computational analysis of the lean-burn direct-injection jet ignition hydrogen engine. *Proc. Inst. Mech. Eng. - Part D J. Automob. Eng.* 224 (2), 261–269. <https://doi.org/10.1243/09544070jauto1278>.
- Brinks, H., Hektor, E.A., 2020. Ammonia as a marine fuel. In: *Assessment of Selected Alternative Fuels and Technologies*.
- Busch, P., Kendall, A., Lipman, T., 2023. A systematic review of life cycle greenhouse gas intensity values for hydrogen production pathways. *Renew. Sustain. Energy Rev.* 184, 113588. <https://doi.org/10.1016/j.rser.2023.113588>.
- Camacho, M.d. I.N., Jurburg, D., Tanco, M., 2022. Hydrogen fuel cell heavy-duty trucks: review of main research topics. *Int. J. Hydrogen Energy* 47 (68), 29505–29525. <https://doi.org/10.1016/j.ijhydene.2022.06.271>.
- Carlisle, D.P., Feetham, P.M., Wright, M.J., Teagle, D.A., 2023. Public response to decarbonisation through alternative shipping fuels. *Environ. Dev. Sustain.* 1–20.
- Charnews, D.P., 2009. *Marine Diesel Engines*. Schiffer+ ORM.
- David, W., 2020. Ammonia: zero-carbon fertiliser, fuel and energy store. Policy Briefing.
- Dedes, E., Hudson, D., Turnock, S., 2016. Investigation of diesel hybrid systems for fuel oil reduction in slow speed ocean going ships. *Energy* 114, 444–456. <https://doi.org/10.1016/j.energy.2016.07.121>.
- Dell, R.M., Bridger, N.J., 1975. Hydrogen—the ultimate fuel. *Appl. Energy* 1 (4), 279–292. [https://doi.org/10.1016/0306-2619\(75\)90029-X](https://doi.org/10.1016/0306-2619(75)90029-X).
- Di Natale, F., Carotenuto, C., 2015. Particulate matter in marine diesel engines exhausts: emissions and control strategies. *Transport. Res. Transport Environ.* 40, 166–191. <https://doi.org/10.1016/j.trd.2015.08.011>.
- Edwards, R., Larivé, J.-F., Rickeard, D., Weindorf, W., 2014. Well-To-Tank Report Version 4.0: JEC well-to-wheels Analysis.
- Ekmekçioglu, A., Kuzu, S.L., Ünlügençoglu, K., Çelebi, U.B., 2020. Assessment of shipping emission factors through monitoring and modelling studies. *Sci. Total Environ.* 743, 140742. <https://doi.org/10.1016/j.scitotenv.2020.140742>.
- Erans, M., Sanz-Pérez, E.S., Hanak, D.P., Clulow, Z., Reiner, D.M., Mutch, G.A., 2022. Direct air capture: process technology, techno-economic and socio-political challenges. *Energy Environ. Sci.* 15 (4), 1360–1405. <https://doi.org/10.1039/d1ee03523a>.
- Fenton, D.L., Khan, A.S., Kelley, R.D., Chapman, K.S., 1995. *Combustion Characteristics Review of ammonia-air Mixtures*. American Society of Heating, Refrigerating and Air-Conditioning Engineers, pp. 1–2505.
- Flannery, J.F., 1925. The diesel engine in navigation. *J. Roy. Soc. Arts* 73 (3771), 339–363 [Online]. Available: <http://www.jstor.org/stable/41357671>.
- Fletcher, M.E., 1975. From coal to oil in British shipping. *J. Transport Hist.* ss-3 (1), 1–19. <https://doi.org/10.1177/002252667500300101>.
- Forby, N., Thomsen, T.B., Cordtz, R.F., Bræstrup, F., Schramm, J., 2023. Ignition and combustion study of premixed ammonia using GDI pilot injection in CI engine. *Fuel* 331, 125768. <https://doi.org/10.1016/j.fuel.2022.125768>.
- Fu, Z., et al., 2023. Fuel cell and hydrogen in maritime application: a review on aspects of technology, cost and regulations. *Sustain. Energy Technol. Assessments* 57, 103181.
- Fumey, B., Buetler, T., Vogt, U.F., 2018. Ultra-low NOx emissions from catalytic hydrogen combustion. *Appl. Energy* 213, 334–342. <https://doi.org/10.1016/j.apenergy.2018.01.042>.
- Gomes Antunes, J.M., Mikalsen, R., Roskilly, A.P., 2009. An experimental study of a direct injection compression ignition hydrogen engine. *Int. J. Hydrogen Energy* 34 (15), 6516–6522. <https://doi.org/10.1016/j.ijhydene.2009.05.142>.
- Gössling, S., Meyer-Habighorst, C., Humpe, A., 2021. A global review of marine air pollution policies, their scope and effectiveness. *Ocean Coast Manag.* 212, 105824. <https://doi.org/10.1016/j.ocecoaman.2021.105824>.
- Griffiths, D., 1997. British marine industry and the diesel engine. *The Northern Mariner/Le marin du nord* 7 (3), 11–40.
- Hall, C.A., Lambert, J.G., Balogh, S.B., 2014. EROI of different fuels and the implications for society. *Energy Policy* 64, 141–152.
- S. O.E. Hansen. "#PoweredByBallard: The first hydrogen-powered vessels set sail." BALLARD. <https://blog.ballard.com/marine/first-hydrogen-powered-vessels-marine> (accessed 12/06/2023).
- Hinić, V., Radica, G., Jurić, Z., Lalić, B., Vidović, T., 2025. Performance analysis of hybrid marine energy systems. *Transp. Res. Procedia* 83, 178–185. <https://doi.org/10.1016/j.trpro.2025.02.025>.
- Huang, L., et al., 2021. Experimental study on piloted ignition temperature and auto ignition temperature of heavy oils at high pressure. *Energy* 229, 120644.
- IEC 62282-3-100:2019 Fuel Cell Technologies, 2020. I. E. Commission [Online]. Available: <https://webstore.iec.ch/en/publication/59566>.
- I.M.O., 2023. Reduction of GHG emissions from SHIPS: report of the fifteenth meeting of the intersessional working group on reduction of GHG emissions from ships (ISWG-GHG 15). In: MARINE ENVIRONMENT PROTECTION COMMITTEE (MEPC) 80th Session, Agenda Item 7, 2023. [Online]. Available: <https://www.imo.org/en/MediaCentre/PressBriefings/pages/Revised-GHG-reduction-strategy-for-global-shipping-adopted.aspx>.
- ISO 3046-1:2002 reciprocating internal combustion engines — performance, I. S. Organisation [Online]. Available: <https://www.iso.org/standard/28330.html>.
- Jeon, J., Kim, S.J., 2020. Recent progress in hydrogen flammability prediction for the safe energy systems. *Energies* 13 (23), 6263. <https://doi.org/10.3390/en13236263>.
- Jones, L.W., 1971. Liquid hydrogen as a fuel for the future: replacement of hydrocarbon fuel for transportation systems by liquid hydrogen is proposed and discussed. *Science* 174 (4007), 367–370.
- Karvounis, P., Theotokatos, G., Vlaskos, I., Hatziaepostolou, A., 2023. Methanol combustion characteristics in compression ignition engines: a critical review. *Energies* 16 (24), 8069 [Online]. Available: <https://www.mdpi.com/1996-1073/16/24/8069>.
- Kaur, D., Singh, M., Singh, S., 2022. 24 - lithium-sulfur batteries for marine applications. In: Gupta, R.K., Nguyen, T.A., Song, H., Yasin, G. (Eds.), *Lithium-Sulfur Batteries*. Elsevier, pp. 549–577.
- Kennerley, A., 2008. Stoking the boilers: firemen and trimmers in British merchant ships, 1850–1950. *Int. J. Marit. Hist.* 20 (1), 191–220. <https://doi.org/10.1177/084387140802000110>.
- Kersey, J., Popovich, N.D., Phadke, A.A., 2022. Rapid battery cost declines accelerate the prospects of all-electric interregional container shipping. *Nat. Energy* 7 (7), 664–674. <https://doi.org/10.1038/s41560-022-01065-y>.
- Khoa, N.X., Lim, O., 2022. Influence of combustion duration on the performance and emission characteristics of a spark-ignition engine fueled with pure methanol and ethanol. *ACS Omega* 7 (17), 14505–14515. <https://doi.org/10.1021/acsomega.1c05759>.
- Kurz, R., et al., 2022. Chapter 6 - transport and storage. In: Brun, K., Allison, T. (Eds.), *Machinery and Energy Systems for the Hydrogen Economy*. Elsevier, pp. 215–249.
- Laasma, A., Otsason, R., Tapaninen, U., Hilmola, O.-P., 2022. Evaluation of alternative fuels for coastal ferries. *Sustainability* 14 (24), 16841 [Online]. Available: <http://www.mdpi.com/2071-1050/14/24/16841>.
- Laboratory, N.E.T., Energy, U.S.D., 2005. *Fuel Cell Handbook*. University Press of the Pacific.
- Larminie, J., Dicks, A., McDonald, M.S., 2003. *Fuel Cell Systems Explained*. J. Wiley, Chichester, UK.
- Lasocki, J., Bednarski, M., Sikora, M., 2019. Simulation of ammonia combustion in dual-fuel compression-ignition engine. In: *IOP Conference Series: Earth and Environmental Science*, 214. IOP Publishing, 012081.
- Lee, S.J., Yi, H.S., Kim, E.S., 1995. Combustion characteristics of intake port injection type hydrogen fueled engine. *Int. J. Hydrogen Energy* 20 (4), 317–322. [https://doi.org/10.1016/0360-3199\(94\)00052-2](https://doi.org/10.1016/0360-3199(94)00052-2).
- Liu, Jie, et al., 2010. Effect of pilot diesel quantity and fuel delivery advance angle on the performance and emission characteristics of a methanol-fueled diesel engine. *Energy Fuels* 24 (3), 1611–1616.
- Mallouppas, G., Yfantis, E.A., 2021. Decarbonizing in shipping industry: a review of research, technology development, and innovation proposals. *J. Mar. Sci. Eng.* 9 (4), 415. <https://doi.org/10.3390/jmse9040415>.
- Manias, P., McKinlay, C., Teagle, D.A., Hudson, D., Turnock, S., 2024. A wind-to-wake approach for selecting future marine fuels and powertrains. *Int. J. Hydrogen Energy* 82, 1039–1050.
- Marine power generation system 200 [Online]. Available: <https://powercellgroup.com/product/marine-system-200/>.
- Maugh, T.H., 1972. Hydrogen: synthetic fuel of the future. *Science* 178 (4063), 849–852. <https://doi.org/10.1126/science.178.4063.849>.
- Mauler, L., Duffner, F., Zeier, W., Leker, J., 2021. Battery cost forecasting: a review of methods and results with an outlook to 2050. *Energy Environ. Sci.* 14. <https://doi.org/10.1039/D1EE01530C>.
- McKinlay, C., 2023. *Dynamic Energy System Modelling to Assess Viable zero-emission Shipping Solutions*. University of Southampton.
- McKinlay, C.J., Turnock, S.R., Hudson, D.A., 2021a. Route to zero emission shipping: hydrogen, ammonia or methanol? *Int. J. Hydrogen Energy* 46 (55), 28282–28297.
- McKinlay, C.J., Turnock, S., Hudson, D., 2021b. Fuel cells for shipping: to meet on board demand and reduce emissions. *Energy Rep.* 7, 63–70.
- McKinlay, C., Manias, P., Turnock, S.R., Hudson, D., 2022a. Dynamic modelling of ammonia crackers and hydrogen PEM fuel cells for shipping applications. *ICCAS*. <https://doi.org/10.3940/rina.iccas.2022.22>.
- McKinlay, C., Turnock, S., Hudson, D., Manias, P., 2022b. Alternative shipping fuels: modelling wind-farm-to-wake emissions. *Scaling Decarbonisation Solutions*.
- McKinlay, C.J., Turnock, S.R., Hudson, D.A., Manias, P., 2024. Hydrogen as a deep sea shipping fuel: modelling the volume requirements. *Int. J. Hydrogen Energy* 69, 863–873. <https://doi.org/10.1016/j.ijhydene.2024.05.054>.
- Melideo, D., Desideri, U., 2024. The use of hydrogen as alternative fuel for ship propulsion: a case study of full and partial retrofitting of roll-on/roll-off vessels for short distance routes. *Int. J. Hydrogen Energy* 50, 1045–1055. <https://doi.org/10.1016/j.ijhydene.2023.10.142>.
- Melsted, O., Pallua, I., 2018. The historical transition from coal to hydrocarbons: previous explanations and the need for an integrative perspective. *Can. J. Hist.* 53 (3), 395–422. <https://doi.org/10.3138/cjh.ach.53.3.03>.
- Meyer, P.E., Winebrake, J.J., 2009. Modeling technology diffusion of complementary goods: the case of hydrogen vehicles and refueling infrastructure. *Technovation* 29 (2), 77–91.
- Mi, S., et al., 2023. Potential of ammonia energy fraction and diesel pilot-injection strategy on improving combustion and emission performance in an ammonia-diesel dual fuel engine. *Fuel* 343, 127889. <https://doi.org/10.1016/j.fuel.2023.127889>.
- Micoli, Luca, Coppola, Tommaso, Turco, Maria, 2021. A case study of a solid oxide fuel cell plant on board a cruise ship. *J. Mar. Sci. Appl.* 20 (3), 524–533.
- Muratori, M., Bush, B., Hunter, C., Melaina, M.W., 2018. Modeling hydrogen refueling infrastructure to support passenger vehicles. *Energies* 11 (5), 1171 [Online]. Available: <https://www.mdpi.com/1996-1073/11/5/1171>.
- Mylonopoulos, F., Durgaprasad, S., Coraddu, A., Polinder, H., 2024. Lifetime design, operation, and cost analysis for the energy system of a retrofitted cargo vessel with

- fuel cells and batteries. *Int. J. Hydrogen Energy* 91, 1262–1273. <https://doi.org/10.1016/j.ijhydene.2024.10.235>.
- Nadimi, E., Przybyla, G., Lewandowski, M.T., Adamczyk, W., 2023. Effects of ammonia on combustion, emissions, and performance of the ammonia/diesel dual-fuel compression ignition engine. *J. Energy Inst.* 107, 101158. <https://doi.org/10.1016/j.joei.2022.101158>.
- Ng, C.K.L., Liu, M., Lam, J.S.L., Yang, M., 2023. Accidental release of ammonia during ammonia bunkering: dispersion behaviour under the influence of operational and weather conditions in Singapore. *J. Hazard Mater.* 452, 131281. <https://doi.org/10.1016/j.jhazmat.2023.131281>.
- Niki, Y., Nitta, Y., Sekiguchi, H., Hirata, K., 2019. Diesel fuel multiple injection effects on emission characteristics of diesel engine mixed ammonia gas into intake air. *J. Eng. Gas Turbines Power* 141 (6). <https://doi.org/10.1115/1.4042507>.
- Nikolaides, P., Poullikkas, A., 2017. A comparative overview of hydrogen production processes. *Renew. Sustain. Energy Rev.* 67, 597–611.
- Ning, G., Haran, B., Popov, B.N., 2003. Capacity fade study of lithium-ion batteries cycled at high discharge rates. *J. Power Sources* 117 (1), 160–169. [https://doi.org/10.1016/S0378-7753\(03\)00029-6](https://doi.org/10.1016/S0378-7753(03)00029-6).
- Pagliaro, M., 2020. 18 - hydrogen-powered boats and ships. In: Iulianelli, A., Basile, A. (Eds.), *Current Trends and Future Developments on (Bio-) Membranes*. Elsevier, pp. 411–419.
- Paul, D., 2020. "A history of electric ship propulsion systems. *IEEE Ind. Appl. Mag.* 26 (6), 9–19. <https://doi.org/10.1109/MIAS.2020.3014837> [History].
- Pedersen, K.A., Lewandowski, M.T., Schulze-Netzer, C., Pasternak, M., Løvås, T., 2023. Ammonia in dual-fueled internal combustion engines: impact on NOx, N2O, and soot formation. *Energy Fuel* 37 (22), 17585–17604. <https://doi.org/10.1021/acs.energyfuels.3c02549>.
- PemGen MT-FCPI-600 [Online]. Available: <https://nedstack.com/sites/default/files/2023-04/mt-fcpi-600.pdf>.
- Pfromm, P.H., 2017. Towards sustainable agriculture: fossil-free ammonia. *J. Renew. Sustain. Energy* 9 (3). <https://doi.org/10.1063/1.4985090>.
- Powertrain, M., MAHLE jet ignition. Available in: <https://www.mahlepowertrain.com/en/experience/mahle-jet-ignition/>. Last accessed: September, 2023.
- Psarrafis, H.N., Lyridis, D.V., Kontovas, C.A., 2012. The economics of ships. In: *The Blackwell Companion to Maritime Economics*, pp. 371–391.
- Ritari, A., Huotari, J., Tammi, K., 2023. Marine vessel powertrain design optimization: multiperiod modeling considering retrofits and alternative fuels. *Proc. IME M J. Eng. Marit. Environ.* 237 (3), 597–614. <https://doi.org/10.1177/14750902221145747>.
- Scharl, T.S.V., 2022. Ignition and combustion characteristics of diesel piloted ammonia injections. *Fuel Communications* 11.
- S.E.M.T. PIELSTICK, 1995. In: PIELSTICK, S.E.M.T. (Ed.), *Marine propulsion systems*, 12–95, p. 313.
- Service, R.F., 2018. Liquid Sunshine. American Association for the Advancement of Science.
- Sheldon, D., 2017. Methanol production-a technical history. *Johnson Matthey Technology Review* 61 (3), 172–182.
- Shudo, T., 2007. Improving thermal efficiency by reducing cooling losses in hydrogen combustion engines. *Int. J. Hydrogen Energy* 32 (17), 4285–4293. <https://doi.org/10.1016/j.ijhydene.2007.06.002>.
- Sørensen, B., 1991. A history of renewable energy technology. *Energy Policy* 19 (1), 8–12. [https://doi.org/10.1016/0301-4215\(91\)90072-V](https://doi.org/10.1016/0301-4215(91)90072-V).
- Sundén, B., 2019. Fuel cell systems and applications. *Hydrogen, Batteries and Fuel Cells*. Elsevier, pp. 203–216.
- Sutton, M., 2023. Manufacturing grins: the gazoo racing-developed gr corolla and yaris are transforming the way toyota builds performance cars. *Car Driv.* 69 (4), 60–66.
- Svanberg, M., Ellis, J., Lundgren, J., Landäl, I., 2018. Renewable methanol as a fuel for the shipping industry. *Renew. Sustain. Energy Rev.* 94, 1217–1228. <https://doi.org/10.1016/j.rser.2018.06.058>.
- Swider, A., Pedersen, E., 2018. Data-driven methodology for the analysis of operational profile and the quantification of electrical power variability on marine vessels. *IEEE Trans. Power Syst.* 34 (2), 1598–1609.
- Szalek, A., Pielecha, I., Cieslik, W., 2021. Fuel cell electric vehicle (FCEV) energy flow analysis in real driving conditions (RDC). *Energies* 14 (16), 5018 [Online]. Available: <https://www.mdpi.com/1996-1073/14/16/5018>.
- Tang, Y., Yuan, W., Pan, M., Li, Z., Chen, G., Li, Y., 2010. Experimental investigation of dynamic performance and transient responses of a kW-class PEM fuel cell stack under various load changes. *Appl. Energy* 87 (4), 1410–1417. <https://doi.org/10.1016/j.apenergy.2009.08.047>.
- Tashie-Lewis, B.C., Nnabuife, S.G., 2021. Hydrogen production, distribution, storage and power conversion in a hydrogen economy - a technology review. *Chem. Eng. J. Adv.* 8, 100172. <https://doi.org/10.1016/j.cej.2021.100172>.
- Taylor, C.F., 1985. *Internal combustion engine in theory and practice*, revised. In: *Combustion, Fuels, Materials, Design*, ume 2. MIT press.
- Teuchies, J., Cox, T.J.S., Van Itterbeeck, K., Meysman, F.J.R., Blust, R., 2020. The impact of scrubber discharge on the water quality in estuaries and ports. *Environ. Sci. Eur.* 32 (1), 103. <https://doi.org/10.1186/s12302-020-00380-z>.
- Thomas, G., 2006. Potential Roles of Ammonia in a Hydrogen Economy. <http://www.hydrogen.energy.gov/pdfs/nh3.paper.pdf>.
- Thomas, H., 2018. Options for Producing low-carbon Hydrogen at Scale.
- Vega-Garita, V., Alpizar-Gutierrez, V., Calderon-Obaldia, F., Núñez-Mata, O., Arguello, A., Immonen, E., 2024. Iterative sizing methodology for photovoltaic plants coupled with battery energy storage systems to ensure smooth power output and power availability. *Energy Convers. Manag.* X 24, 100716. <https://doi.org/10.1016/j.ecmx.2024.100716>, 2024/10/01/.
- Ventayol, A.A., Lam, J.S.L., Bai, X., 2025. Comparative life cycle assessment of hydrogen internal combustion engine and fuel cells in shipping. *Int. J. Hydrogen Energy* 109, 774–788.
- Verhelst, S., Wallner, T., 2009. Hydrogen-fueled internal combustion engines. *Prog. Energy Combust. Sci.* 35 (6), 490–527. <https://doi.org/10.1016/j.pecs.2009.08.001>.
- Wärtsilä 25DF product guide [Online]. Available: <https://www.wartsila.com/marine/products/engines-and-generating-sets/dual-fuel-engines/wartsila-25>.
- Welch, A., Wallace, J., 1990. Performance characteristics of a hydrogen-fueled diesel engine with ignition assist. *Alternative Diesel Fuels* 227.
- White, C.M., Steeper, R.R., Lutz, A.E., 2006. The hydrogen-fueled internal combustion engine: a technical review. *Int. J. Hydrogen Energy* 31 (10), 1292–1305. <https://doi.org/10.1016/j.ijhydene.2005.12.001>.
- Wilcox, J., Psarras, P.C., Liguori, S., 2017. Assessment of reasonable opportunities for direct air capture. *Environ. Res. Lett.* 12 (6), 065001. <https://doi.org/10.1088/1748-9326/aa6de5>.
- Wimmer, A., Wallner, T., Ringler, J., Gerbig, F., 2005. H2-direct injection—a highly promising combustion concept. *SAE Technical Paper*, pp. 148–7191.
- Wouters, C., Burkardt, P., Steeger, F., Fleischmann, M., Pischinger, S., 2023. Comprehensive assessment of methanol as an alternative fuel for spark-ignition engines. *Fuel* 340, 127627. <https://doi.org/10.1016/j.fuel.2023.127627>.
- Xing, H., Stuart, C., Spence, S., Chen, H., 2021. Fuel cell power systems for maritime applications: progress and perspectives. *Sustainability* 13 (3), 1213 [Online]. Available: <https://www.mdpi.com/2071-1050/13/3/1213>.
- Xu, L., Xu, S., Bai, X.-S., Repo, J.A., Hautala, S., Hyvönen, J., 2023. Performance and emission characteristics of an ammonia/diesel dual-fuel marine engine. *Renew. Sustain. Energy Rev.* 185, 113631. <https://doi.org/10.1016/j.rser.2023.113631>.
- Yang, Z.L., et al., 2012. Selection of techniques for reducing shipping NOx and SOx emissions. *Transport. Res. Transport Environ.* 17 (6), 478–486. <https://doi.org/10.1016/j.trd.2012.05.010>.
- Younas, M., Shafique, S., Hafeez, A., Javed, F., Rehman, F., 2022. An overview of hydrogen production: current status, potential, and challenges. *Fuel* 316, 123317. <https://doi.org/10.1016/j.fuel.2022.123317>.
- Younkins, M., Boyer, B., Wooldridge, M., 2013. Hydrogen DI dual zone combustion system. *SAE International Journal of Engines* 6 (1), 45–53. <https://doi.org/10.4271/2013-01-0230>.
- Zamfirescu, C., Dincer, I., 2008. Using ammonia as a sustainable fuel. *J. Power Sources* 185 (1), 459–465. <https://doi.org/10.1016/j.jpowsour.2008.02.097>.
- Zhang, F., Shuai, S., Wang, Z., Zhang, X., Wang, J., 2011. A detailed oxidation mechanism for the prediction of formaldehyde emission from methanol-gasoline SI engines. *Proc. Combust. Inst.* 33 (2), 3151–3158. <https://doi.org/10.1016/j.proci.2010.07.029>.

**Panos Manias MEng** is a research assistant for the Southampton Marine and Maritime Institute, with his main focus being decarbonisation of shipping through the utilisation of alternative fuels and powertrains. At the same time, he is a final year PhD student with his thesis aim being the efficient and safe utilisation of hydrogen on board ships.

**Professor Stephen Turnock** is Head of Engineering at the University of Southampton. He has long standing interests in decarbonisation of shipping and in particular analysis and modelling of alternative power trains including the use of hybrid battery systems.

**Professor Dominic Hudson** is the Shell Professor of Ship Safety and Efficiency at the University of Southampton. He has research interests in all aspects of ship hydrodynamics, particularly ship design and operation for energy efficiency.

**Professor Damon A.H. Teagle** Professor of Geochemistry in the School of Ocean & Earth Science at the University of Southampton and has sailed on numerous oceanographic cruises, many as chief scientist. Until Aug 2025 he was Director of the Southampton Marine & Maritime Institute that pulls together multi-disciplinary ocean-facing expertise from across the University of Southampton. He has particular interest in maritime decarbonisation and the integration of green shipping-port energy systems and operations.